République Algérienne Démocratique et Populaire
Ministère de l'Enseignement Supérieur
et de la Recherche Scientifique
Université Aboubakr Belkaid
Tlemcen

Faculté des Sciences
Département de Physique

Thèse de Doctorat d'Etat
Es-Sciences Physiques

Présentée par

Mme Benmouna Farida Née Benachenhou

Sur le thème

Diagrammes de Phases des Mélanges de Polymères et Cristaux Liquides

le 21 NOVEMBRE 1999
Devant le jury

Monsieur le Professeur : **Baba Ahmed**	**Abdellatif**	Président
Monsieur le Professeur : **Guermouche**	**Hacène**	Examinateur
Monsieur le Professeur : **Belbachir**	**Ahmed**	Examinateur
Monsieur le Professeur : **Benyoucef**	**Boumediène**	Examinateur
Monsieur le Professeur : **Benmouna**	**Mustapha**	Rapporteur

ACKNOWLEDGEMENTS

This work has been accomplished in collaboration with Dr. Ulrich Maschke and Prof. Xavier Coqueret of the University of Lille in France. I am particulary indebted to Dr. Maschke for all the efforts he made to make this collaboration successful. Without his enthousiasm this thesis would not have been implemented in such good conditions. I thank Prof. Xavier Coqueret for his hospitality as the director of the Laboratoire de Chimie Macromoléculaire de Lille and enlightning discussions during my stays in his laboratory. Part of this work has been made in collaboration with Prof. Jean–Marc Buisine and his collaborators at the Université du Littoral (Dunkerque) and in particular Dr. Frédérick Roussel and Dr. Abdelylah Daoudi. I would like to express my deepest gratitude to all of them for their active contribution in the experimental part of this work.

I would like to thank all the members of this commitee for their interest in this work and for taking the time to read it and judge it.

PREFACE

This thesis contains two parts. The first part describes the theoretical model used to establish the phase diagrams of mixtures of polymers and liquid crystals. It gives the basic concepts governing the phase behavior of these mixtures in the presence of nematic or smectic A order. The concepts are put forward using mean field models which are well documented in the literature. In the isotropic state, the thermodynamics are essentially contained in the theories of Flory and coworkers of polymer statistics. The free energy in the isotropic state which is the starting point in the description of the thermodynamic properties depends crucially upon the architecture of the polymer and the isotropic interaction between different species present in the mixture. We tried to describe the extend to which the polymer architecture and in particular the presence of crosslinks in the network influences the phase behavior of mixtures of high molecular weight polymers and low molecular weight liquid crystals. A comparative analysis of the phase behavior with linear chains and crosslinked polymer networks is given. An attempt is made to characterize the effect of crosslinks on the phase diagram. We discussed in some detail the models for the elastic free energy and rubber elasticity parameters. Other chain architecture can be easily considered within the same theoretical framework. A particular attention has also been given to the Flory-Huggins interaction parameter which governs the miscibility in the isotropic state. This parameter is assumed to be function of temperature and composition of the mixture. The thermodynamic properties of ordered phases are described by classical mean field theories. If the order is of the nematic type the corresponding free energy is given by the Maier-Saupe theory in terms of an orientational order parameter of the small liquid crystal molecules with respect to a reference axis. The strength of nematic interaction is proportional to the quadrupole interaction parameter which in turn is proportional to the ratio of the temperature of the system and the nematic-isotropic

transition temperature characteristic of the liquid crystal under investigation. We also consider the case of liquid crystals having in addition to the orientation nematic order, a directional smectic-A order. In this case, one has stacks of layers of nematic ordered liquid crystal molecules along the z axis with a certain periodicity. The theory of smectic-A order has been developed by McMillan as a generalization of the Maier-Saupe theory. It induces a second order parameter which takes into account the layer structure of the ordered phase. A parameter describing the strength of the potential of mean field in the smectic phase is introduced. This parameter depends on the smectic-nematic transition temperature characteristic of the liquid crystal. Another class of systems is studied in the first part dealing with mixture of nematogens. Here we consider the case of polymers carrying side chain rigid groups having a nematic order. The phase properties of these mixtures are completely different from those of single nematogen systems. Their phase diagrams have quite different shapes and exhibit a rich variety of coexisting phases. The theory for these systems was developed first by Brochard and coworkers in the case of intermediate nematogen coupling and later by Kyu and coworkers who included the influence of nematogen coupling. Our main contribution is to generalize this theory to systems where the polymer matrix is made of a crosslinked network. Not only we have developed the theoretical framework for this generalization but we also demonstrated its applicability to real systems. We have undergone an experimental study to describe the phase properties of various mixtures having either a single nematic component or a smectic-A liquid crystal. We considered also the case of nematogen mixtures. We used several experimental techniques to construct the phase diagrams such as optical polarized microscopy, differential scanning calorimetry and light scattering. We were able to analyze our experimental data quite successfully for practically all the systems. Recently we started an experimental program using crosslinked polymers prepared by an unique technique using

electron beam irradiation. In all the cases known in the literature so far the curing of samples was made using UV irradiation. The EB curing technique has the particular advantage of leading to samples with a much better quality in terms of crosslinking efficiency. We expect that this will enable us to characterize unambiguously the effect of crosslinking on the phase behavior of polymers and liquid crystal mixtures.

This thesis represents only a limited part of a research program which we implemented during the last years. We have chosen deliberately two chapters in this program to give an idea about the theoretical achievement made and the experimental proofs we have given to the usefullness of the theory we developed. Other investigations made within the framework of this program were published in various journals or are waiting publication. The list of these papers will be given as an appendix to this thesis.

PART 1

EQUILIBRIUM PHASE BEHAVIOR OF POLYMER AND LIQUID CRYSTAL BLENDS

SUMMARY

A theoretical framework describing the equilibrium phase behavior of polymers and liquid crystals is presented. Linear and crosslinked polymers are considered and complexities found in the phase properties of systems involving crosslinked networks are highlighted. Effects of the rubber elasticity parameters in the elastic free energy are found to induce substantial distorsions in the phase diagram. The Flory-Huggins interaction parameter which governs the miscibility of the mixture in the isotropic state is modelled either by assuming that it is function of temperature only or temperature and composition.

The thermodynamic description of the ordered domains is made according to the Maier-Saupe theory for nematic order and its extension to include other ordering properties. In particular, the smectic A order is described according to the generalization of the Maier-Saupe theory proposed by McMillan. In the presence of nematogens, the coupling leads to quite different phase properties. In the strong coupling limit, a wide single nematic phase is found. In the weak coupling, the miscibility gap is much wider. These mixtures are described with mean field theories of nematogen first developed by Brochard et al. and later extended by Kyu et al.. This theoretical formalism has been applied successfully to analyze data obtained on several systems including linear and crosslinked polymer networks, smectic and nematic LMWLC, and nematogen mixtures.

1. Introduction

The phase behavior of polymers and liquid crystals (LCs) is the subject of a growing interest for various reasons. From a fundamental point of view, it raises basic questions concerning the phase properties of multicomponent systems with widely different characteritics. From the point view of their applications, these systems are useful in various fields such as display technology and privacy windows[1-6]. The progress made recently in understanding the effect of architecture on the thermodynamics of polymer blends and in elucidating the physics of LC has provided new incentives for putting more effort in investigating these systems[7-12]. These efforts are now paving the way for further achievements.

The knowledge of the phase properties of these mixtures is a crucial step towards a better understanding of their performance under real conditions. This knowledge is necessary in the process of promoting new applications or designing new materials. For practical and economic reasons, one seeks large ordered monodomains in the host medium. One way to achieve this goal is to reduce the quantity of LC dissolved in the polymer matrix collecting the maximum amount of LC in the ordered domains. The quantity remaining in the polymer rich phase acts as a plasticizer reducing the polymer glass transition temperature. The decrease of T_g results not only into a lower mechanical strength of the polymer but also changes the optical properties and modifies the refractive index matching of the polymer and the ordinary component of the LC. The latter condition is dictated by the need to reach a maximum transmission of light in the electro-optical response of the system[3-6,13]. Several parameters control the miscibility of the mixture besides the nature and the architecture of the polymer. For linear chains, it is known that the miscibility decreases with increasing molecular weight. The miscibility in the isotropic state is mainly controlled by the interaction parameter χ[14]. In addition to depending on the nature of

monomers building the chains, χ can be function of temperature and composition as well. Assuming that χ depends on temperature only is sometimes not sufficient to describe the experimental data. The polymer architecture has a large impact upon the miscibility of the polymer/LC system. In the present work, a particular attention is given to the phase properties of linear polymers and corresponding crosslinked networks mixed with low molecular weight liquid crystals (LMWLCs). It was shown that the complexity is much less for linear polymers comparatively to the case of crosslinked chains[12,15-21] where there are more model dependent parameters to be defined. The increased elasticity of the network and the restoring forces at the crosslinks introduce qualitative changes to the phase behavior when polymer and LC are mixed. The higher the crosslinking density, the lower is the average number of monomers between consecutive crosslinks N_c and the lower is the miscibility with the solvent. A description of the phase behavior of the crosslinked polymer and the solvent requires the definition of the rubber elasticity parameters α and β and the polymer volume fraction at crosslinking φ_0. The former parameters are model dependent and can be either constant or function of the composition. The polymer volume fraction at crosslinking φ_0 or the reference state volume fraction has also a certain influence on the phase behavior. Several situations can be considered. If crosslinking is made in the bulk, one has φ_0=1. If another molecular species is present in the initial mixture together with the polymer prior to crosslinking, then φ_0 takes a constant value inferior to 1. If crosslinking takes place in-situ, then φ_0 remains equal to the polymer volume fraction φ_2. The effect of the crosslinking density and reference state volume fraction on the phase properties of the mixture are somewhat correlated.

The systems studied here are characterized by either nematic or smectic-A orders. Several examples will be considered. Systems made of flexible polymers and nematic LMWLC are investigated first. A comparison is made of the phase behavior of mixtures involving either

a linear polymer or a crosslinked network. Changes in the phase diagrams when the LMWLC presents both a nematic and a smectic-A order are analyzed. If the polymer has side chain nematogen groups, its phase properties in the presence of a LMWLC are completely modified as compared to the single nematic systems. There is an important change in the ordering properties when the rigid molecules are attached to the chain backbone. Not only the transition temperature from the isotropic state to the nematic order is modified but the miscibility with either an isotropic solvent or an anisotropic LMWLC is different. Even if the rigid side chain groups and the LMWLC molecules are chemically identical, they may exhibit a large degree of incompatibility. Phase diagrams of side chain liquid crystal (SCLC) polymers and isotropic solvents are completely different from those of polymers and LMWLC. In binary nematogen mixtures, one finds a variety of phase diagrams depending on the extend of coupling. In the presence of a strong coupling, a new single nematic order different from the individual nematic phases appears signaling a high miscibility of the nematogens. A smectic order may be induced in the strong nematic coupling but this will not be considered here. The free energy of nematic order is modeled according to the Maier-Saupe theory[22,23]. When smectic A order appears, its description is made following the McMillan theory[24].

In this paper we present the theoretical formalism describing the phase behavior of systems exhibiting different structures. The thermodynamics in the isotropic state for both linear and crosslinked polymer networks in the presence of low molecular weight solvents are analyzed. This description is based upon the Flory-Huggins lattice model[14] for linear chains and the Flory-Rehner theory[14,25,26] of rubber elasticity for crosslinked polymers along with extensions for the rubber elasticity parameters.

The application of this formalism to mixtures similar to others used in the literature is presented. A brief comparison of theoretical predictions and experimental data is given.

2. Flory-Huggins and Flory-Rehner theories of isotropic mixing

2.1. Free energies

In order to analyze the phase behavior of mixtures of polymers and LC it is necessary to characterize their thermodynamics in the isotropic state. This can be done starting from a free energy model appropriate for the system under consideration. Throughout this paper we deal with mixtures of two components. One is the high molecular weight polymer and the other is the low molecular weight solvent or LC. We will deal with polymers made of linear flexible chains having N_2 repeat units and with the case of crosslinked networks. The latter can be viewed as a single molecule with a total number of n_2 repeat units. In each system, the solvent or the LC molecule is made of N_1 repeat units. The thermodynamics of these systems in the presence of a LC either in the isotropic or in the nematic state show different features. In the good solvent conditions, linear polymers exhibit a single homogenous phase while the presence of crosslinks introduces an upper bound to the swelling of the network. Even under good solvent conditions, a phase separation takes place at the network saturation and a pure solvent phase emerges in equilibrium with a swollen polymer network.

The case of a linear polymer

In the case of a polymer-solvent binary solution, the free energy density (per unit volume or unit site) is given by the Flory Huggins model[14)]

$$\frac{f^{(I)}}{k_B T} = \frac{\varphi_1}{N_1}\ln\varphi_1 + \frac{\varphi_2}{N_2}\ln\varphi_2 + \chi\varphi_1\varphi_2 \qquad (1)$$

where the subscripts 1 and 2 refer to the solvent and the polymer, respectively. For convenience, it will be assumed that all units occupy the same reference volume and hence the volume fractions φ_1 and φ_2 are

$$\varphi_1 = \frac{n_1 N_1}{n_0} = 1 - \varphi_2 \qquad (2)$$

n_1 and n_2 are the number of molecules of type 1 and 2, respectively. n_0 is the total number of repeat units in the system $n_0 = n_1 N_1 + n_2 N_2$; χ is the Flory-Huggins interaction parameter.

The phase behavior of this system in the isotropic state is described within the Flory-Huggins lattice model by the three parameters N_1, N_2, and χ. The entropic penalty when N_1 and/or N_2 increase induces a strong miscibility loss. Increasing χ also results into enhanced tendancy towards phase separation. In the case where the polymer is a crosslinked network, there are several parameters to be defined in order to proceed with the description of the phase behavior and hence it is certainly more complicated.

The case of a crosslinked polymer

The swelling behavior of the crosslinked polymer in the low molecular weight solvent depends on the elasticity of the network. The isotropic free energy density is a sum of two contributions.

$$f^{(i)} = f^{(e)} + f^{(m)} \qquad (3)$$

The first contribution is the elastic free energy density $f^{(e)}$ which in the framework of the Flory-Rehner theory[14,25,26] is given by

$$\frac{f^{(e)}}{k_B T} = \frac{3\alpha\varphi_0^{2/3}}{2N_c}\left[\varphi_2^{1/3} - \varphi_2\right] + \frac{\beta\varphi_2}{N_c}\ln\varphi_2 \qquad (4)$$

The rubber elasticity parameters α and β are model dependent. According to James and Guth[27], α=1 and β=0 while Flory[28] suggests to let α=1 and β=2/f, f being the functionality of the monomers. Petrovic[29] suggested that α and β are function of the monomer functionality and the polymer volume fraction according to

$$\alpha = \frac{f-2+2\varphi_2}{f}, \quad \beta = \frac{2\varphi_2}{f} \tag{5}$$

In equation 4, N_c is the average number of repeat units between consecutive crosslinks and is a measure of the crosslinking density. The elastic free energy shows the complexity of the crosslinked polymer as compared to the linear polymer problem. In addition to the quantities N_c and φ_0, one has to make a choice for the parameters α and β. Further difficulties come from the fact that the elastic free energy is often written in another form, leading to a different influence of φ_0. Indeed, the following elastic free energy is also used[30,31)]

$$\frac{f^{(e)}}{k_B T} = \frac{3\alpha}{2N_c}\left[\varphi_0^{2/3}\varphi_2^{1/3} - \varphi_2\right] + \frac{\beta\varphi_2}{N_c}\ln\left(\frac{\varphi_2}{\varphi_0}\right) \tag{6}$$

Equations 4 and 6 lead to the same result if φ_0=1. Discrepancies appear if crosslinking takes place in the polymer bulk. More importantly, the latter model fails in the situation of in-situ polymerization and crosslinking where $\varphi_0=\varphi_2$. If φ_0 is a constant between 0 and 1, the two elastic free energies differ only slightly at weak and moderate crosslinking. If the crosslinking is high, discrepancies are more significant.

The second contribution to the isotropic free energy of equation 3 is given by the energy of mixing

$$\frac{f^{(m)}}{k_B T} = \frac{\varphi_1 \ln\varphi_1}{N_1} + \chi\varphi_1\varphi_2 \tag{7}$$

In principle the χ-parameter depends on the polymer architecture and hence should be different whether one deals with a linear or a crosslinked polymer. Such differences due to the polymer architecture are not completely eludicidated and the problem remains quite challenging of properties of polymer systems.

The Flory-Huggins interaction parameter χ is allowed to be function of temperature T and volume fraction φ_2 according to[32-34)]

$$\chi = \chi_0 + \chi_1\varphi_2 + \chi_2\varphi_2^2 \tag{8}$$

where χ_0 is function of temperature

$$\chi_0 = A + \frac{B}{T} \tag{9}$$

χ_1 and χ_2 are either constant or function of temperature. This interaction parameter is commonly used in the literature. It could be useful in the interpretation of experimental data under certain conditions. The effect of other parameters such as molecular weight, polydisperse

e parameters A, B, χ_1, and χ_2.

g the chemical potentials of components 1

otentials are

(10)

s are kept constant in the derivation, and

s sometimes convenient to express the

free energy density $\frac{\partial f}{\partial \varphi_2}$. It is easy to

(11)

(12)

μ_1 is given by equation 11 but μ_2 is slightly adapted to the network which can be viewed as a single molecule

$$\mu_2 = f - \varphi_1 \frac{\partial f}{\partial \varphi_1} \tag{13}$$

2.3. Phase diagrams

There are two methods to construct the bihodal curves : either graphically using the double tangent method or analytically by equating the chemical potentials of constituants 1 and 2 in the coexisting phases denoted by primes and double primes. Here, it is the latter method which is adopted by solving numerically the set of equations

$$\mu_1^{(\prime)} = \mu_1^{(\prime\prime)} \tag{14}$$

$$\mu_2^{(\prime)} = \mu_2^{(\prime\prime)} \tag{15}$$

According to equations 11 to 13, the latter set is simplified for both linear and crosslinked polymers and becomes

$$f - \varphi_2 \left.\frac{\partial f}{\partial \varphi_2}\right|' = f - \varphi_2 \left.\frac{\partial f}{\partial \varphi_2}\right|'' \tag{16}$$

$$\left.\frac{\partial f}{\partial \varphi_2}\right|' = \left.\frac{\partial f}{\partial \varphi_2}\right|'' \tag{17}$$

The spinodal line defines the extension of unstable regions and is given by equating the second derivative of the free energy to zero, i. e.

$$\frac{\partial^2 f}{\partial \varphi_2^2} = 0 \tag{18}$$

This procedure is the same in the isotropic state and in the presence of nematic or smectic order using the free energy corresponding to the system under consideration. The following section gives two particular examples of isotropic systems involving either a linear or a crosslinked polymer.

2.4. Applications

Figure 1 represents the phase diagrams of binary mixtures consisting of linear polymers with two values of N_2 and a low molecular weight solvent. As pointed out earlier, this species is assumed to have a single repeat unit and N_1=1. The interaction parameter for isotropic mixing is modeled in two different ways. One way considers that this parameter is function of temperature only. This leads to the two phase diagrams displayed in the lower part of the figure. The second way is to assume that χ is function of temperature and composition. This leads to the two phase diagrams in the upper part of figure 1.

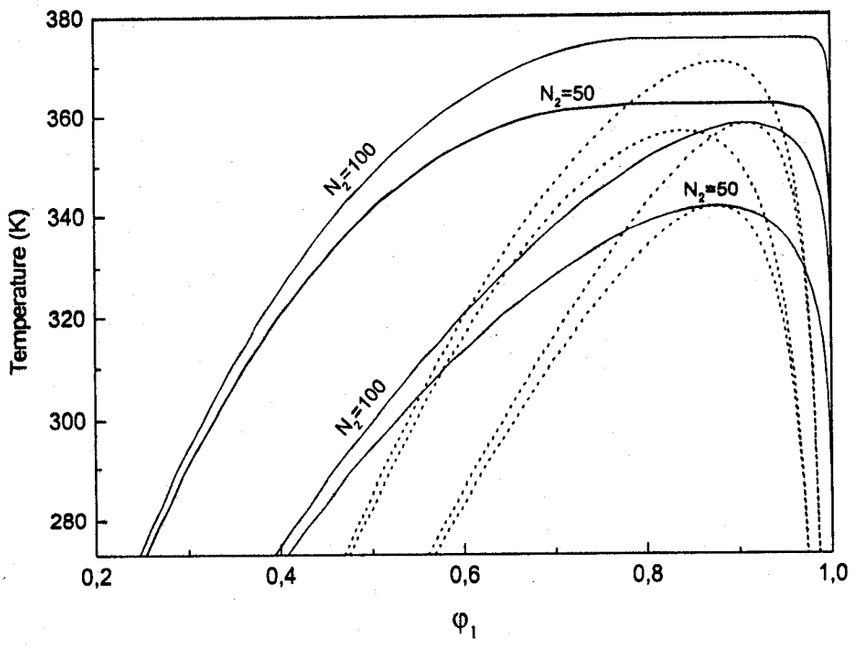

Figure 1

Phase diagram of a linear polymer/solvent isotropic mixture for N_1=1, two values of N_2 and two models for the Flory-Huggins interaction parameter. The solid curve represents the binodals and the dashed curve represents the spinodals. In the descending order, these diagrams correspond to N_2=50, χ=-0.35+342/T+0.3φ_2+0.04φ_2^2; N_2=10 and the same χ-parameter ; N_2=50, χ=-0.35+342/T ; N_2=10 and the same χ-parameter.

In all cases one obtains typical upper critical solution temperature diagrams (UCST) with the solid lines representing coexistence curves and the dashed lines are spinodals. In the case where χ is function of temperature only following equation 9 the spinodal is given by

$$T_c = 2B\left[\frac{1}{N_1\varphi_1}+\frac{1}{N_2\varphi_2}-2A\right]^{-1} \tag{19}$$

If χ depends on temperature and composition according to equation 8, the spinodal equation becomes

$$T_c = 2B\left[\frac{1}{N_1\varphi_1}+\frac{1}{N_2\varphi_2}-2\left(A+\chi_1\varphi_2+\chi_2\varphi_2^2\right)\right]^{-1} \tag{20}$$

The isotropic-isotropic miscibility gap I+I becomes wider as N_2 increases. One observes that in the diagrams where χ is function of composition, there is no critical point. Furthermore, the maximum of the coexistence curve tends to broaden with an enhanced tendancy for the higher polymer molecular weight. In the case where the critical point exists and χ is function of temperature only, the coordinates of the critical points φ_c and T_c increase with N_2. Within the meanfield approximation T_c is given by equation 19 and φ_c is expressed in terms of N_1 and N_2 by

$$\varphi_C = \frac{\sqrt{N_2}}{\sqrt{N_1}+\sqrt{N_2}} \tag{21}$$

For mixtures involving crosslinked polymers, the phase diagram is quite different. As mentioned earlier thermodynamic description is comparatively more difficult primarily because of the elastic free energy. A model of rubber elasticity should be choosen to describe the elastic bounds imposed by the crosslinks to the expansion of the polymer. Here we use the classical model for the free energy starting from the Flory-Rehner theory of rubber elasticity. A similiar method as in the case of linear polymers is used leading to the phase diagram of figure 2.

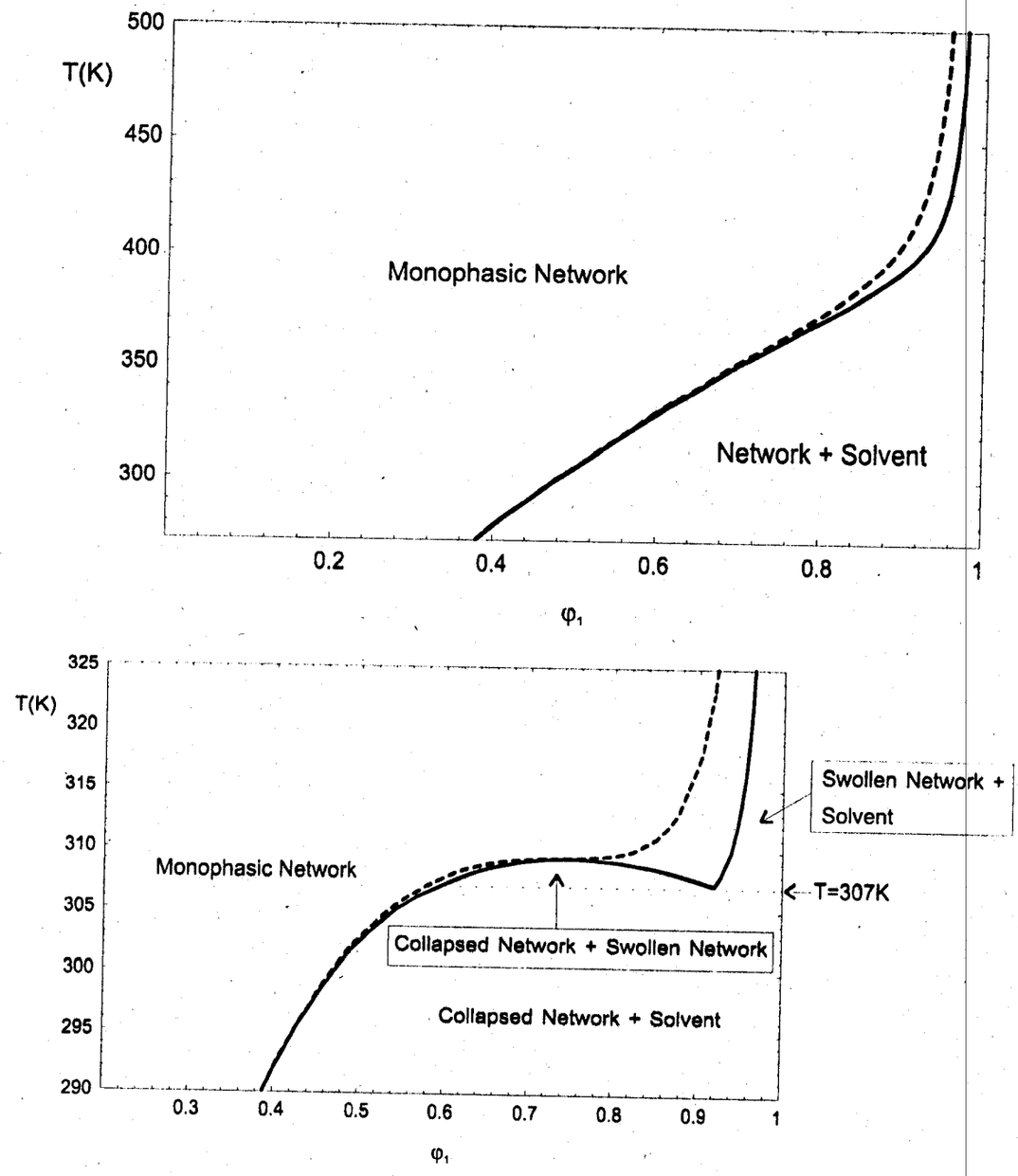

Figure 2

a) Phase diagrams of a crosslinked polymer/solvent isotropic mixture. The dashed curve corresponds to α=1and β=1/2 while the continuous curve corresponds to α=[f-2+2φ_2]/f and β=2φ_2/f. In both diagrams we used χ=-0.35+342/T, N_1=1, N_c=1000, φ_0=1 and f=3.

b) The same as a) with: $\chi=\chi_0+\chi_1\varphi_2+\chi_2\varphi_2^2$, χ_0=-0.35+342/T, χ_1=0.3, χ_2=0.04.

Figure 2a represents the coexisting curves for a loosely crosslinked polymer with N_c=1000 and two choices of the parameters α and β. The dashed lines correspond to α and β constant whereas the solid lines are obtained in the case where α and β are function of composition. The interaction parameter χ depends on temperature only according to equation 9. The y-axis is extended to high temperatures deliberately to capture the region where discrepancies between the two models of rubber elasticity are more apparent. One finds only small differences in the temperature above 400K. In order to see the effect of the Flory-Huggins interaction parameter χ under similar conditions, we plot in figure 2b the coexisting curves for the same systems allowing χ be function of polymer volume fraction according to equation 8. There is a significant difference with figure 2a showing that the effect of χ is crucial in the determination of the phase behavior of crosslinked polymer/ solvent mixtures. In particular, for the systems where the parameters α, β and χ are all allowed to be function of φ_2. The phase diagram exhibits a triple point at 307K whereby a pure solvent phase is in equilibrium with a swollen network and a collapsed network.

These diagrams were established for a loosely crosslinked polymer corresponding to N_c=1000. For a densely crosslinked polymer, N_c is smaller and the miscibility gap polymer/solvent is larger. On the other hand, the polymer volume fraction at crosslinking φ_0 has an influence on the phase diagram. If φ_0 is constant, its influence is larger when N_c is smaller. A higher value of φ_0 induces a larger miscibility gap.

3. Maier-Saupe –McMillan theories of nematic and smectic-A orders

Phase separated mixtures of polymers and LMWLC show micron-sized domains where the small rigid molecules form ordered phases. For nematic LC, the small molecules are aligned along a reference axis in the z direction with an angular distribution. In addition to the isotropic free energy discussed earlier, one has a contribution due to the nematic

$$Z = \int e^{-U(\theta) / \left(k_B T\right)} \, d(\cos\theta) \tag{27}$$

This shows that the order parameter s can be obtained from the partition function by a simple differentiating

$$s = \frac{\partial \log Z}{\partial m_n} \tag{28}$$

On the other hand, the nematic part of the chemical potential can be obtained from equations 11 to 13 by noting that the derivative of the nematic free energy with respect to composition is

$$\frac{\partial f^{(n)}}{\partial \varphi_2} = \ln Z \tag{29}$$

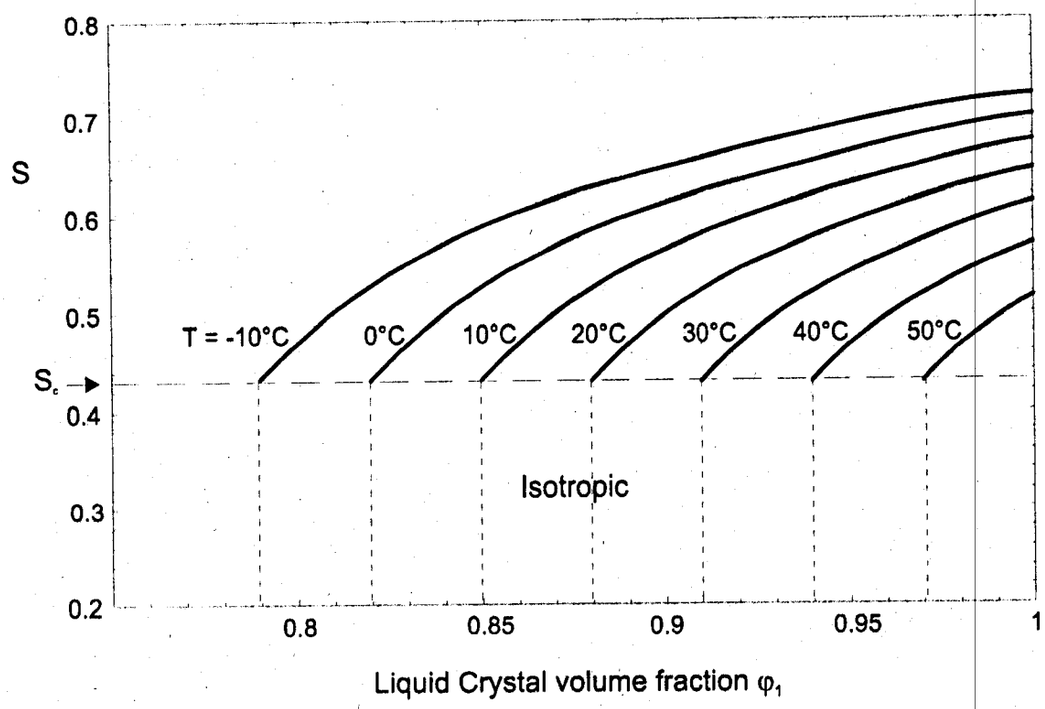

Figure 3

The nematic order parameter s for a polymer/LC mixture as a function of the LC volume fraction φ_1 for several temperatures. From top to bottom, the temperatures are –10, 0, 10, 20, 30, 40, and 50°C, respectively.

Figure 3 shows the variation of the nematic order parameter s as a function of LC volume fraction for different temperatures. It indicates how this parameter increases with the LC composition for temperatures below the nematic-isotropic transtion at T_{NI}=60°C. There is a limiting volume fraction $\varphi_{NI}=T/T_{NI}$ at which the order parameter drops to zero and the system undergoes a first order phase transition. All the ordered domains dispersed in the polymer matrix become isotropic. The variation of the order parameter with composition is not required only for the establishment of the phase diagrams but it is given here because it is useful for a better understanding of the thermodynamic behavior in different regions of the T versus φ_1 phase diagram. An example of this phase diagram is given in figure 4.

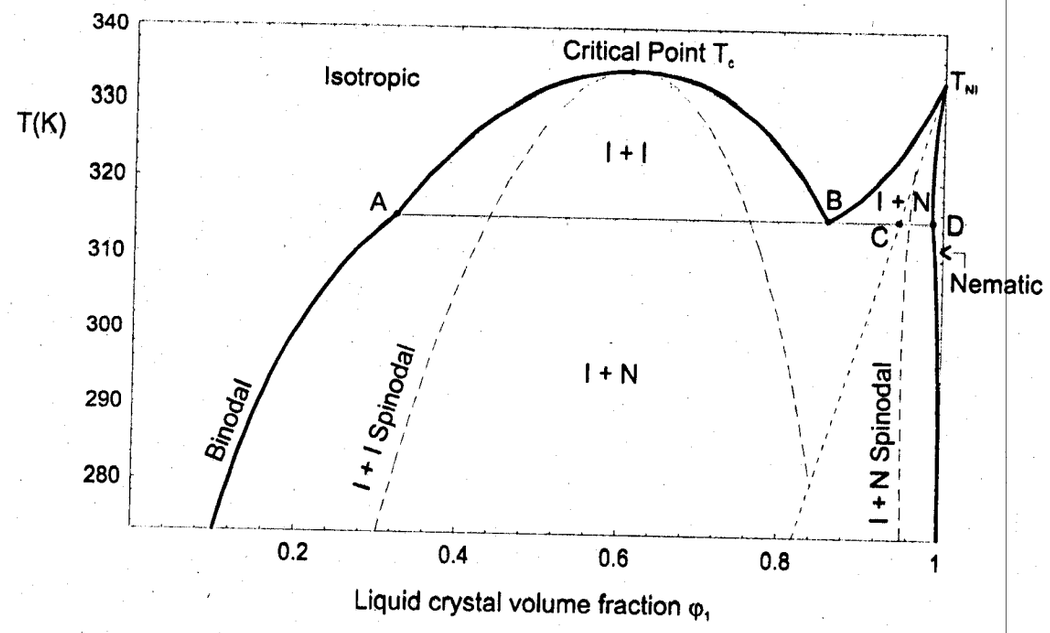

Figure 4

The theoretical phase diagram for a polymer/nematic LMWLC mixture characterized by N_1=4, N_2=10, T_{NI}=60°C and χ=-0.34+225/T. The thick line represents the binodal while the dashed line is the spinodal with its isotropic and nematic branches. I means isotropic and N means nematic. The dotted line represents the variation of the volume fraction at the NI transition with T.

This is a typical phase diagram of a system made of a linear polymer and a nematic LMWLC with T_{NI}=60°C. It is an UCST diagram with a large domain where the system shows a single isotropic phase and with several biphasic regions. It exhibits a triple point at T=42°C where two isotropic phases of different polymer concentrations coexist with a nematic pure LC phase. Above this temperature, the system admits a miscibility gap I+I while below an isotropic polymer rich phase is in equilibrium with a practically pure LC phase in the nematic order. The spinodal curve admits two branches. The isotropic branch ends at the line defined by $\varphi_{NI}=T/T_{NI}$ whereas the nematic branch starts from this line and extends to the region where the LC composition is near φ_1=1. Note that the nematic-isotropic transition temperature T_{NI} chosen here is typical of the eutectic mixture known as E7.

It was observed earlier that the phase diagrams of crosslinked polymers and nematic LC are quite distinct from those of corresponding systems with linear polymers[19]. Figure 5a shows the results for a crosslinked polymer and a nematic LC mixture under similar conditions as figure 4. Several values of N_c are used here to illustrate the effect of crosslinking density. This figure immediately shows the difference with linear polymers. This diagram is much simpler, it exhibits a single isotropic region on the left hand side but in contrast to linear polymer systems, there is a wide miscibility gap I+I on the right hand side above T_{NI}. Below this temperature the miscibility gap consists of an isotropic polymer rich phase coexisting with a pure LC nematic phase and covers a wide range of compositions. As the crosslinking density increases, the number of repeat units between consecutive crosslinks decreases and the I+I miscibility gap becomes wider. To illustrate further the differences of the phase properties of systems involving linear polymers and crosslinked networks, we represent in figure 5b on the same diagram T versus φ_1 the coexistence curves for several values of N_2 and N_c. These two parameters influence the

phase diagram in different ways. While the miscibility is favored when N_2 decreases it is reduced when N_c decreases.

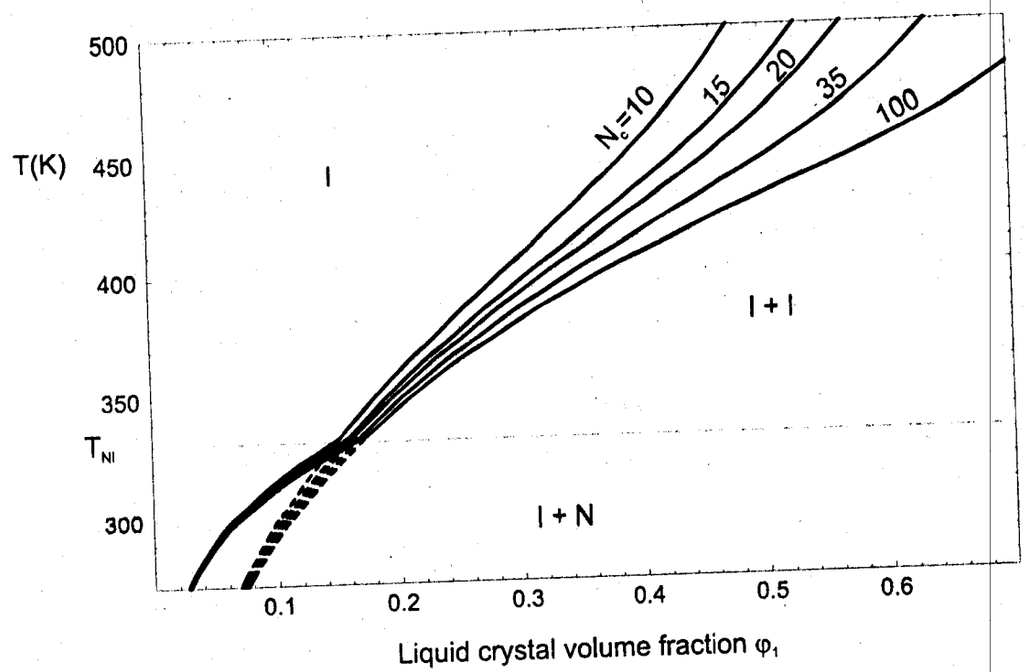

Figure 5

a) Binodals of a polymer/ nematic LMWLC mixture with a crosslinked polymer (N_1=4, χ=-0.34+225/T, T_{NI}=60°C), and N_C=10, 15, 20, 35 and 100 from left to right, respectively. The dashed extensions of the curves correspond to the isotropic case. The range of temperatures has been deliberately extended to 500K to illustrate the effects of crosslinks on the phase diagram of the mixture.

Another example of systems having a nematic order is given by polymers carrying side chain nematogen groups and an isotropic solvent. Both linear polymers with side chain LC and crosslinked polymer networks with side chain LC are considered. The phase properties of these systems are quite different. To illustrate these differences, we represent in figure 6 the phase diagrams of nematic polymers and isotropic solvents for linear polymers (figure 6a) and crosslinked polymers (figure 6b). The difference with the systems where the

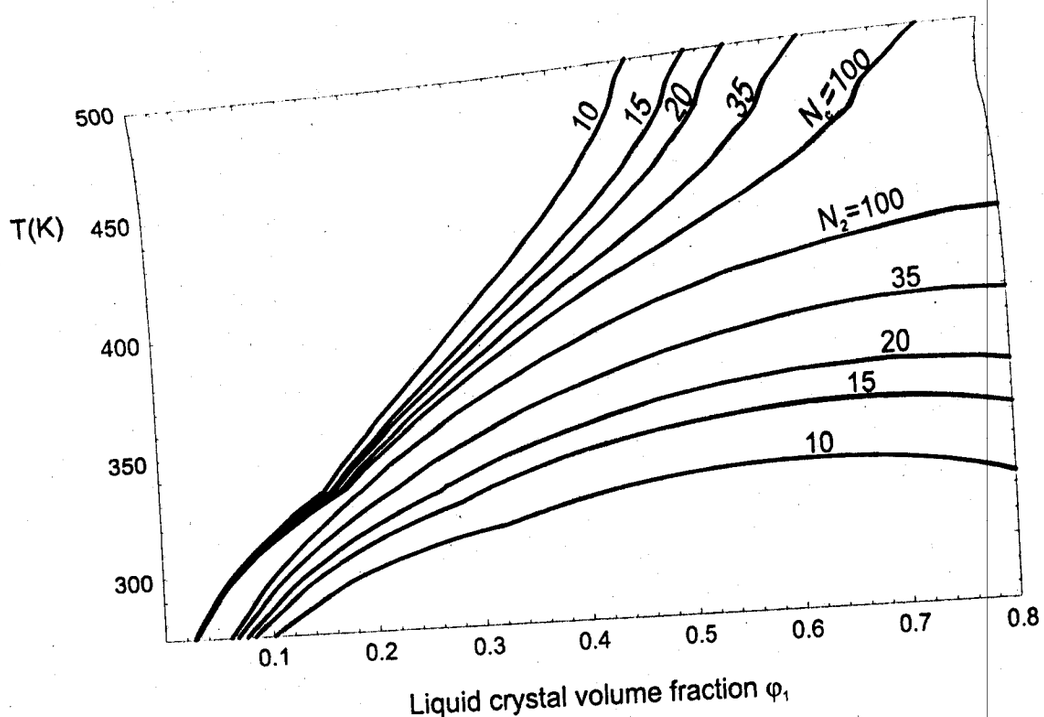

Figure 5

b) Binodals of two polymer/LC systems with and without crosslinks under similar conditions, with N_1=4,χ=-0.34+225/T, T_{NI}=60°C, and N_2= N_C=10, 15, 20, 35 and 100 as indicated on the figure.

polymer is isotropic and the solvent is nematic is clear not only through the inversion of the abscissa axis but through the wide region of a single nematic phase found on the left hand side of this figure. Qualitatively however, the same type of biphasic regions I+I and N+I are encounted whether the LC molecules are free or attached to the polymer backbone.

3.2. Polymer and a LMWLC with a smectic-A order

The Maier-Saupe theory presented above has been extended by McMillan to include the effects of smectic-A order. An additional order parameter σ is introduced to describe the arrangements of LC molecules into stacklayers in the z-direction

$$\sigma = \frac{1}{2}\left\langle \left(3\cos^2\theta - 1\right)\cos\frac{2\pi z}{d}\right\rangle \tag{30}$$

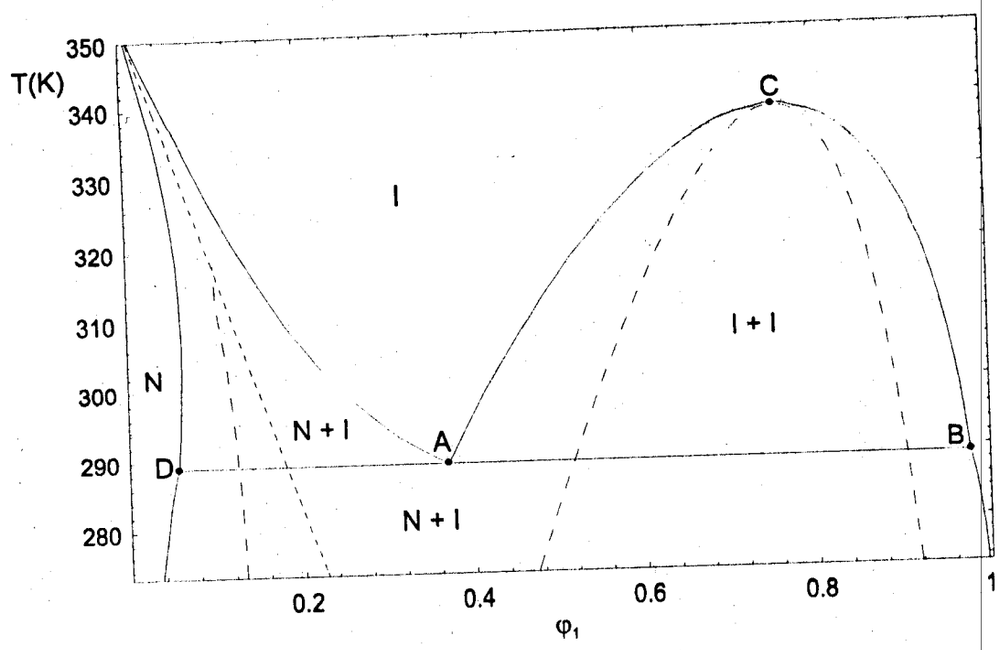

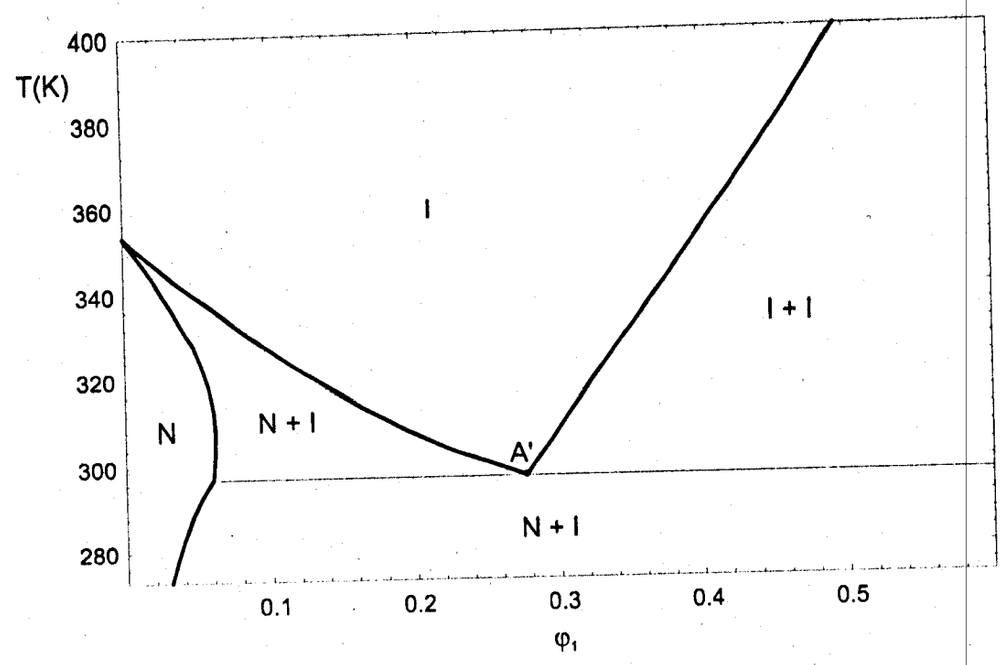

Figure 6

a) **Phase diagram of a SCLCP made of linear chains and a low molecular weight isotropic solvent using** N_1=1, N_2=10, χ=-0.35+408/T, $T_{NI\,2}$=80°C.

b) The same as in a) with a crosslinked polymer network N_C=10.

The free energy is expressed in terms of s and σ as follows

$$\frac{f^{(s)}}{k_B T} = \frac{\varphi_1}{N_1}\left[-\ln Z + \frac{1}{2}\nu\varphi_1(s^2 + \zeta\sigma^2)\right] \tag{31}$$

where the parameter ζ depends on the ratio of the transition temperatures T_{SN}/T_{NI}. In the McMillan theory, ζ increases with T_{SN} towards the limiting value 0.98 when the ratio T_{SN}/T_{NI} reachs one. If ζ is below than 0.98, one has the sequence of transitions smectic to nematic to isotropic and if ζ is equal or higher than 0.98, one has a direct transition from the smectic order to the isotropic state. The smectic partition function Z reads

$$Z = \iint d\mu\, dz \exp\left[\frac{m_n}{2}(3\cos^2\theta - 1)\right]\exp\left[\frac{m_s}{2}(3\cos^2\theta - 1)\cos 2\pi\frac{z}{d}\right] \tag{32}$$

where m_n and m_s are mean field parameters. They can be expressed in terms of s and σ by minimizing the free energy with respect to these order parameters

$$m_n = \nu s\varphi_1 \quad ; \quad m_s = \nu\zeta\sigma\varphi_1 \tag{33}$$

As pointed out earlier the variation of order parameters with temperature and composition is useful for a better understanding of the phase diagram. This variation is given in figure7. Figure 7a corresponds to ζ=0.851 hence to a case where the transition from a smectic to an isotropic phase takes place via a nematic phase. Below T_{SN}, the smectic order parameter decreases with φ_1 and drops to zero at $\varphi_{SN}=T_{SN}/T$. At this composition, the smectic order disappears and the nematic order parameter s undergoes a discontinuous decrease but remains finite. Between T_{SN} and T_{NI}, a nematic order subsists but s decreases with composition until $\varphi_{NI}=T_{NI}/T$ where it undergoes a second discontinuous drop to zero. Figure 7b gives the order parameters for ζ=0.98 corresponding to a direct transition from a smectic-A order to an isotropic state.

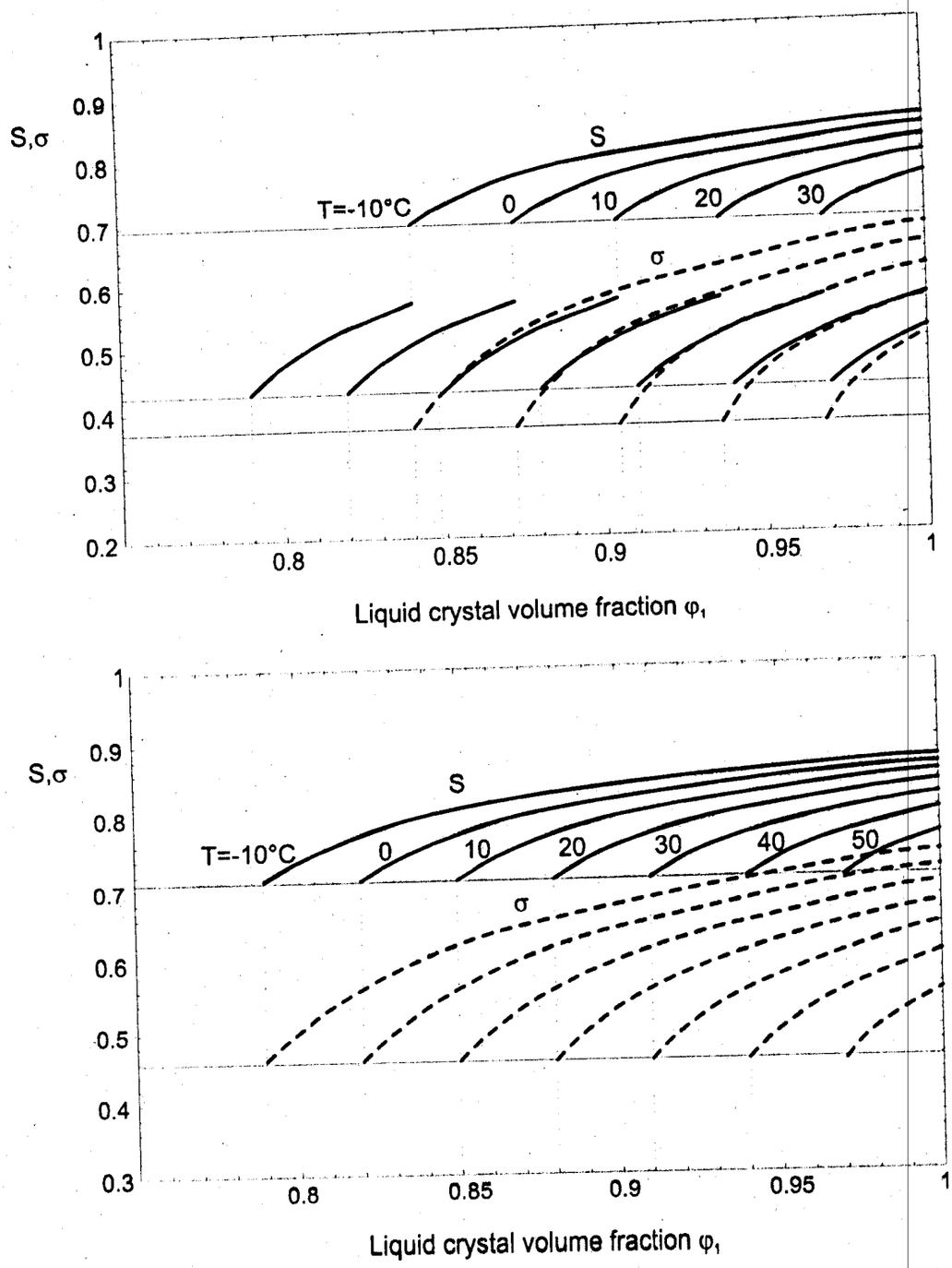

Figure 7

a) Variation of the order parameters s and σ as a function of φ_1 for several temperatures as indicated on the figure, and ζ=0.851 (T_{SN}=40°C). The thick and dashed curves represent s and σ, respectively. The NI transition temperature is T_{NI}=60°C.

b) The same as figure a) for ζ=0.98 and T_{SN}=T_{NI}=60°C.

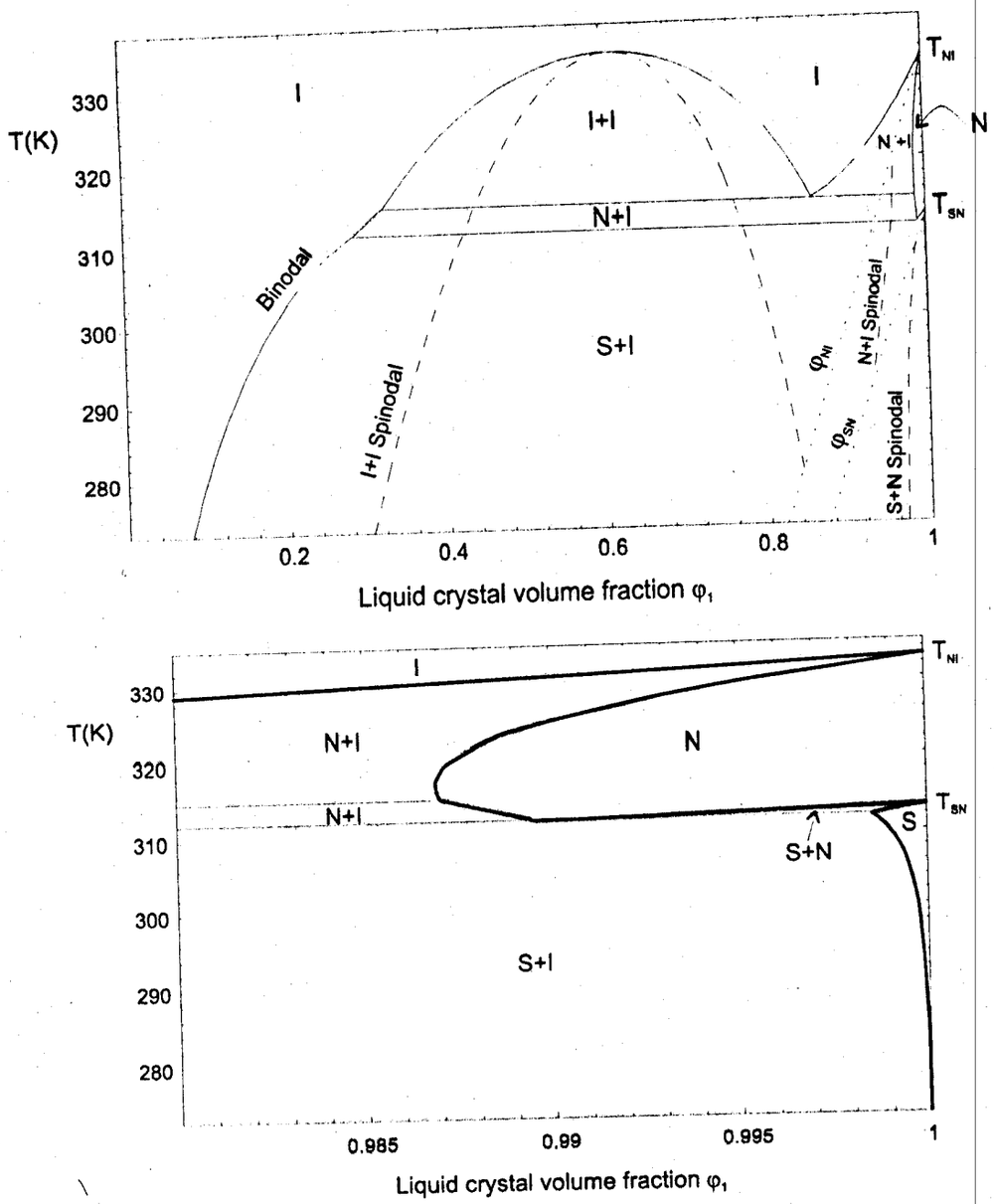

Figure 8

a) Phase diagram of a linear polymer/smectic-A LMWLC mixture using the following parameters : ζ=0.851, T_{SN}=40°C, T_{NI}=60°C, N_1=4, N_2=10, and χ=-0.34+225/T.

b) Enlarged view of figure a) near φ_1=1. The single nematic region above T_{SN} is much wider than the single smectic region.

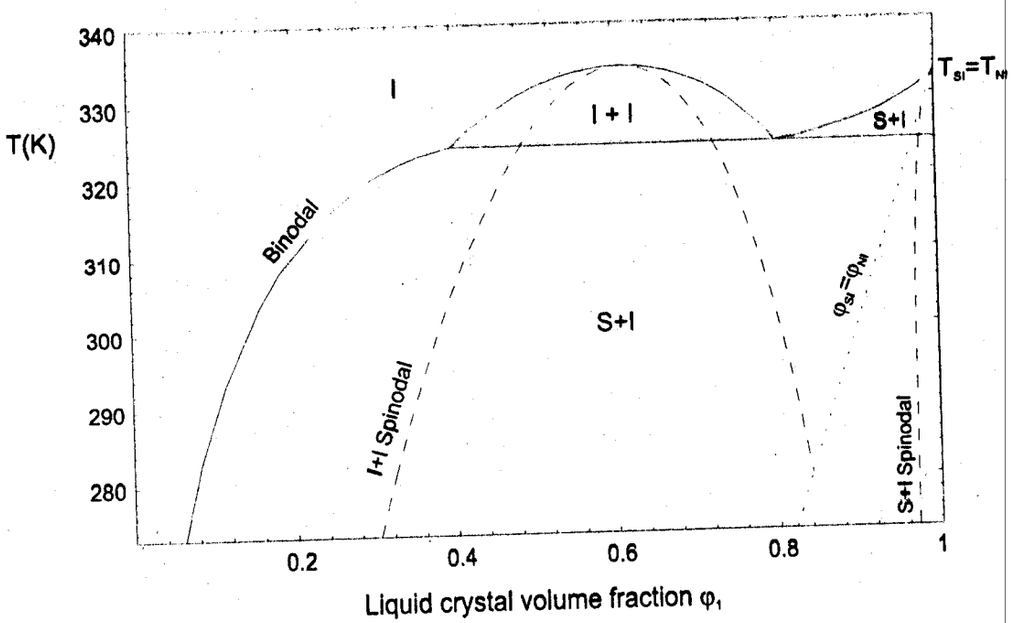

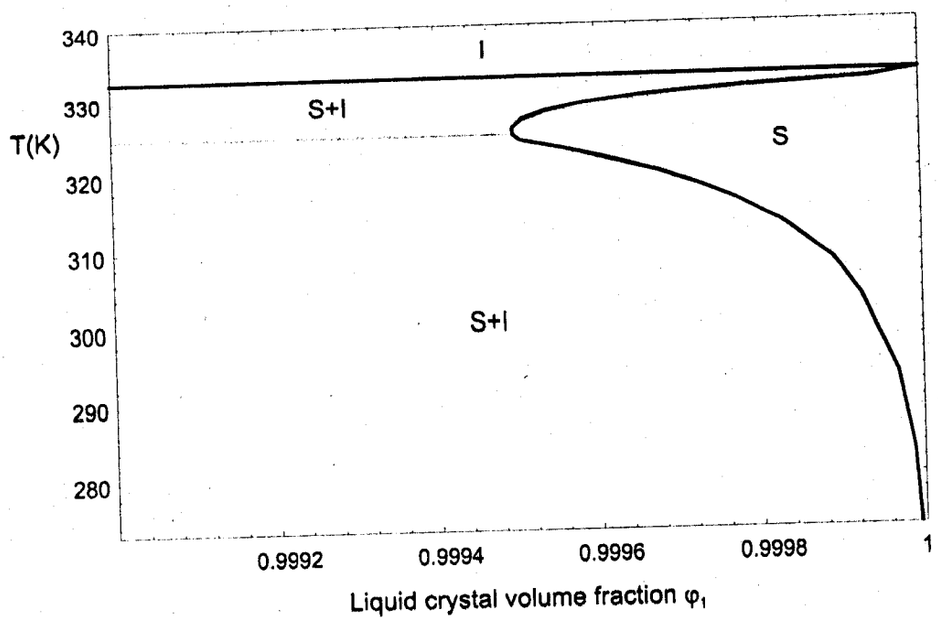

Figure 8

c) Binodal of a linear polymer/smectic-A LMWLC mixture with $T_{NI}=T_{SN}=60°C$, $\zeta=0.98$ and $N_1=4$, $N_2=10$ and $\chi=-0.34+225/T$.

d) Enlarged view of figure c) near $\varphi_1=1$.

These features appear clearly in figure 8 displaying the phase diagrams for the two choices of the smectic parameter ζ and for mixtures involving linear polymers. The amplification of the diagram in the vicinity of φ_1=1 is given in order to highlight the rich phase behavior in this region. In figure 8a and 8b, two triple points exist. The upper one shows two isotropic phases with different polymer concentrations coexisting with a nematic phase. In the lower triple point, an isotropic phase coexists with two LC phases, one isotropic and the other smectic. The diagram in figure 8c and its amplification in figure 8d exhibit only one triple point corresponding to two isotropic phases of different polymer composition in equilibrium with a pure LC smectic phase. No nematic order is found in this case. The smectic order melts down directly into an isotropic state at T_{SI}. These observations are consistent with the variations of the order parameters given in figure 7. The phase behavior is changed quite significantly if, instead of a linear polymer, one deals with a crosslinked network. These discrepancies are highlighted in figure 9a. Interestingly this phase diagram is quite simple. It consists of an isotropic single phase region above the coexistence curve and three distinct biphasic regions below. Below T_{SN}, a pure LC smectic phase coexists with a polymer rich isotropic phase. Between T_{SN} and T_{NI}, a nematic phase is in equilibrium with an isotropic phase while above T_{NI}, an I+I miscibility gap covers a large domain of the temperature versus composition diagram. The effect of the parameter ζ on the phase behavior is given in figure 9b where one sees how the miscibility gap N+I diminishes as ζ increases from 0.851 to 0.98 and the sequence of transitions smectic to nematic to isotropic transforms into a direct melting down of the smectic order into an isotropic phase when T increases above the transition temperature T_{SI}.

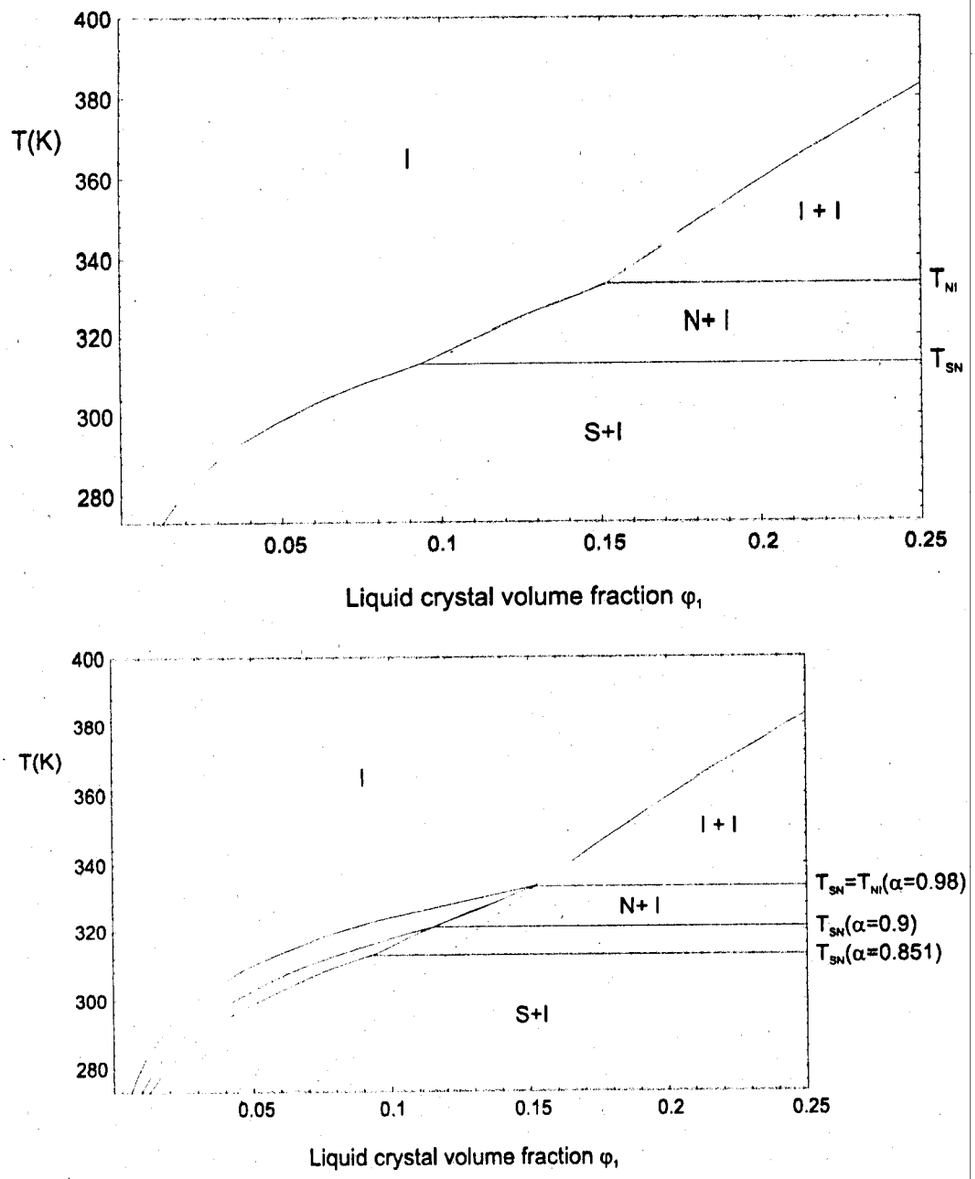

Figure 9

a) The phase diagram for a crosslinked polymer/smectic-A LMWLC mixture with N_c=10, ζ=0.851, T_{SN}=40°C, T_{NI}=60°C, N_1=4 and χ=-0.34+225/T.

b) The same as in a) with three values of ζ. The extension above T_{NI} is the isotropic part and its extension below T_{NI} is represented by a dotted line. The thick curves below T_{NI} are the binodals for ζ=0.98, 0.9 and 0.851 from left to right, respectively.

3.3 Binary nematogen mixtures

These systems are characterized by a rich variety of phase properties. One encounters two types of ordered phases reminiscent of the two molecular species and/or a single ordered phase depending on the strength of coupling between the two nematogens. The isotropic coupling is governed by the Flory-Huggins interaction parameter and its variation with the temperature and composition while the nematic coupling is due to the cross nematic interaction. Here, we ignore the smectic induced order observed experimentally for strongly coupled nematogens. In spite of this simplification we still have a rich variety of phase diagrams. Two nematic-isotropic transition temperatures should be introduced. The first one $T_{NI\,1}$ concerns the LMWLC and the second one is related with the high molecular weight polymer and is denoted $T_{NI\,2}$. This temperature depends not only upon the nature of side chain groups but also on the length and nature of the flexible spacer. According to the rule of Arnold and Zachmann[35,36], one expects a large miscibility of nematogens if the chemical structures of the LMWLC and the side chains are similar. The fact that the rigid molecule is attached to the polymer does not mean that there is a strong coupling with the backbone and hence should not change significantly its anisotropic interaction. However, experimental evidence[37] leads to a different conclusion and reveals that the transition temperature can change by several degrees or even tenth of degrees. Having made these observations, we turn to the model of the free energy required to establish the phase diagram. The nematic contribution to the free energy for the nematogen mixture is given following Brochard et al.[11]

$$\frac{f^{(n)}}{k_B T} = -\varphi_1 \ln Z_1^{(n)} - \varphi_2 \ln Z_2^{(n)} + \frac{1}{2}\left[\nu_{11}\varphi_1^2 s_1^2 + \nu_{22}\varphi_2^2 s_2^2 + 2\nu_{12}\varphi_1\varphi_2 s_1 s_2\right] \tag{34}$$

where the ν_{11} and ν_{22} are the quadrupole interaction parameters for components 1 and 2, respectively and ν_{12} is the cross-interaction term. The former quantities are proportional to

T/T_{NI}, as usual, ν_{11}=4.54 $T/T_{NI\,1}$ and ν_{22}=4.54 $T/T_{NI\,2}$ but the cross term is not known. Brochard et al.[11] suggested that ν_{12} is a geometric mean of the ν's while Kyu et al.[10] proposed to introduce a coupling constant κ such that

$$\nu_{12}^2 = \kappa^2 \nu_{11}\nu_{22} \tag{35}$$

If the phase diagram presents an azeotropic point, Kyu et al. give the method to obtain κ from its composition and temperature. As the coupling parameter κ changes from the strong coupling case (κ>1) to the weak coupling case (κ<1), the phase diagram changes substantially. Binary nematogens are characterized by two order parameters s_1 and s_2 and two partition functions Z_1 and Z_2. These are

$$Z_i^{(n)} = \int \exp\left[\frac{m_i}{2}\left[3\cos^2\theta_i - 1\right]\right] d(\cos\theta_i); \quad i = 1,2 \tag{36}$$

the order parameters can be deduced from Z_1 and Z_2 by a simple differentiation

$$s_i = \frac{\partial \ln Z_i}{\partial m_i}; \quad i = 1,2 \tag{37}$$

where the mean field parameters m_1 and m_2 are obtained by minimization of the free energy with respect to s_1 and s_2

$$m_1 = \nu_{11}\varphi_1 s_1 + \nu_{12}\varphi_2 s_2 \tag{38}$$

$$m_2 = \nu_{22}\varphi_2 s_2 + \nu_{12}\varphi_1 s_1$$

Figure 10 shows the variation of s_1 and s_2 with the temperature and composition for the three cases corresponding to weak coupling (κ=0.851), intermediate coupling (κ=1), and strong coupling (κ =1.15). In the weak coupling case, the order parameter curves show a valley in the variation with the LC volume fraction. Both s_1 and s_2 decrease with φ_1, go through a minimum, then increase. In the intermediate coupling, s_1 and s_2 are very close and follow parallel decrease with φ_1. The strong coupling case gives rise to a different behavior. At low temperatures, the order parameters take large values and change only

slightly. As the temperature increases, they exhibit a maximum. Because of the coupling, s_1 and s_2 take unusual high values as compared to those of the individual nematogens.

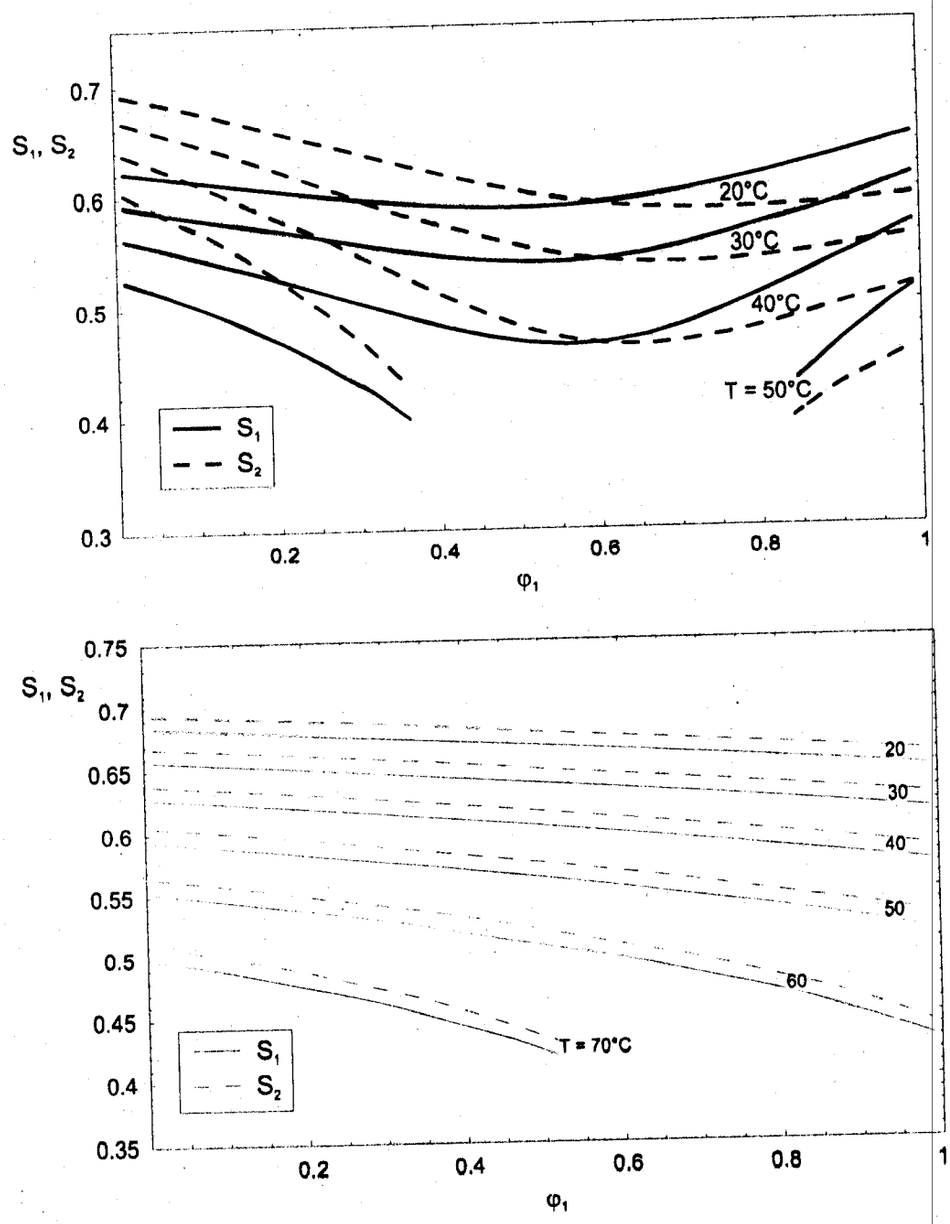

Figure 10

a) Order parameters s_1 (solid curves) and s_2 (dashed curves) versus LMWLC composition for a weak coupling corresponding to κ=0.85. The other parameters are $T_{NI\,1}$=60°C, and $T_{NI\,2}$=80°C.

b) The same as a) for an intermediate nematic coupling corresponding to κ=1.

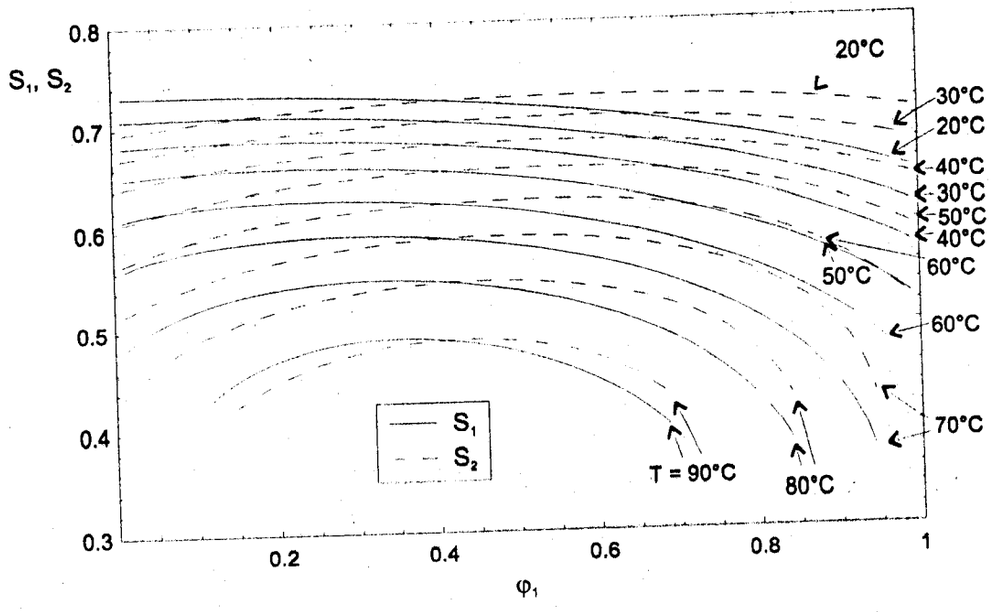

Figure 10

c) The same as a) for a strong nematic coupling corresponding to κ=1.15.

Figure 11 represents the phase diagram of a mixture of side chain LC linear polymer and LMWLC in the weak coupling limit. This figure shows several features illustrating a variety of phase properties. On each side in the temperature composition diagram, it is the majority component which determines the phase behavior of the mixture. Below 50% LC, there is a single nematic phase characteristic of the side chain LC polymer. A tea pot like biphasic region N+I usually found in such nematogen mixtures separates the single nematic from the single isotropic domains. On the right hand side of the figure one recovers phase behavior which is characteristic of the presence of a LMWLC. A narrow region of a single nematic phase N exists. It is separated from the single isotropic phase in the upper part by a small gap of miscibility N+I. This diagram exhibits two triple points designated by dashed lines. The lower triple point corresponds to the coexistence of two nematic phases and a third isotropic phase I. At the upper triple point two isotropic phases with different polymer compositions coexist with a nematic phase. Another interesting

observation is the presence of a large miscibility gap where two nematic phases coexist in the intermediate range of composition, below the temperature of the lower triple point. Between the two dashed lines, a miscibility gap where a nematic phase is in equilibrium with an isotropic phase is found.

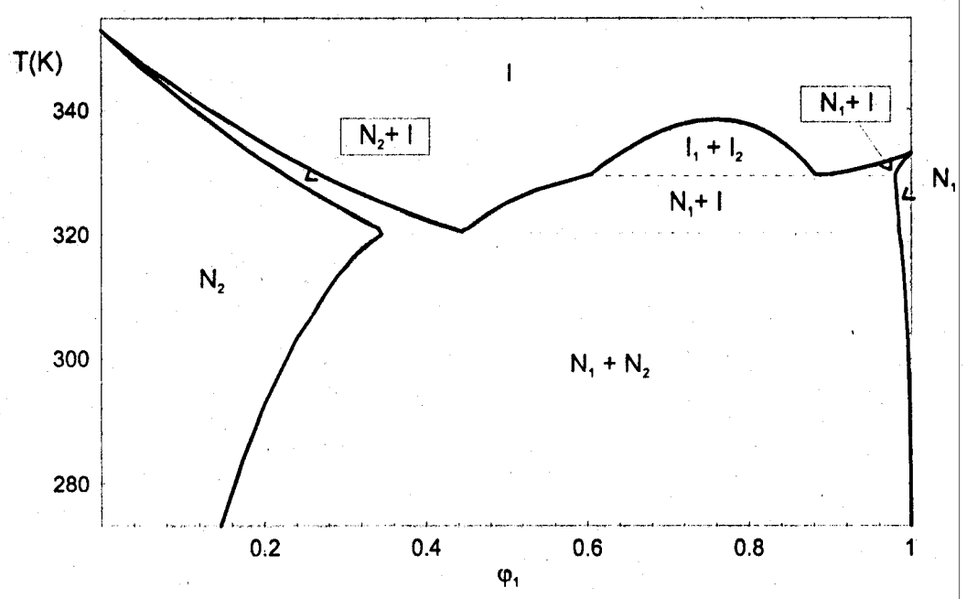

Figure 11

Phase diagram of SCLCP with linear chains and a LMWLC. The parameters of this mixture are N_1=1, N_2=10, χ=-0.35+408/T, κ=0.851 (weak coupling), $T_{NI\ 1}$=60C, and $T_{NI\ 2}$=80C.

In the strong coupling limit of figure 12, the phase behavior looks somewhat simpler. A region of a single nematic phase covers a wide range of temperature and composition. The strong coupling induces a better miscibility of the nematogens in spite of their differences. Starting from the single nematic phase, upon heating there is a very narrow range of temperature where an isotropic phase emerges. Further heating the sample slightly, the whole system melts down into a single isotropic phase. Upon cooling one finds a small range of composition where the mixture separates into two distinct nematic phases. It

would be interesting to check if similar observations could be made in the case of crosslinked polymers with side chain LC.

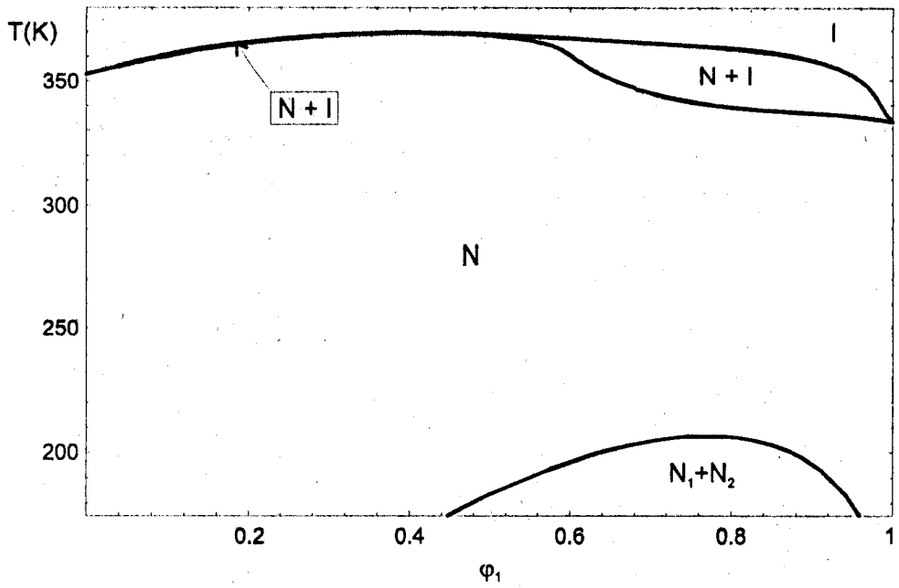

Figure 12

The same as in Figure 11 in the strong nematic coupling represented by κ=1.15. N_1 and N_2 in the lower region of the diagram represent two nematic coexisting phases: N_1=LC rich phase, N_2=SCLCP rich phase.

Figure 13 shows the phase diagram in the weak coupling limit. Obviously this diagram is different from that of figure 11 for a similar mixture involving linear chains. The single nematic phase with a trace amount of polymer does not exist. The I+I miscibility gap is wider and extends to much higher temperatures as compared to linear polymer systems. The single isotropic phase region is significantly reduced.

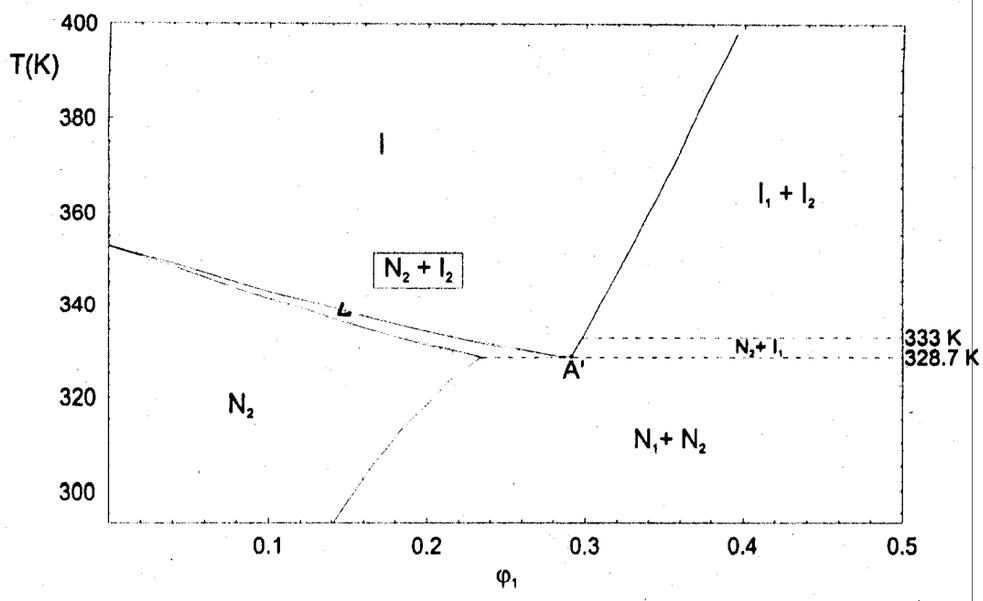

Figure 13

Phase diagram of SCLCP with crosslinked polymer network (N_C=10) and a LMWLC. In addition to the phases already defined, we have in this figure I_1=isotropic pure LC phase, I_2=isotropic polymer rich phase, N_1=nematic pure LC phase. The other parameters of this mixture are N_1=1, χ=-0.35+408/T, κ=0.85 (weak coupling limit), $T_{NI\ 1}$=60C, and $T_{NI\ 2}$=80C.

In the strong coupling limit, the phase diagram is given in figure 14 and does not exhibit a single nematic phase unlike linear polymer systems. This diagram is dominated by the nematic phase characteristic of the side chain LC polymer. The crosslinks introduce an upper limit to the swelling of the polymer leading to the emergence of a pure LMWLC phase. The phase diagram is strongly distorted on the right hand side. The miscibility gap in this part of the figure is extremely large in all biphasic regions whether having two nematic phases, one nematic and the other isotropic or two isotropic phases. Likewise, in the case of strong coupling the right hand side region of the phase diagram is mostly

affected by the presence of crosslinks. The strong coupling modifies remarkably the narrow strip on the left hand side characteristic of tea pot diagrams.

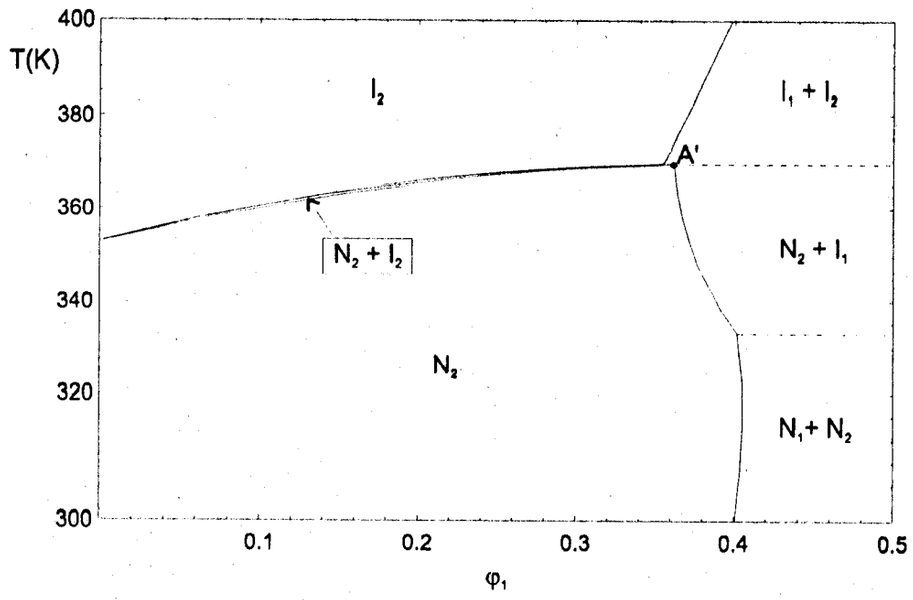

Figure 14

The same as in figure 13 in the strong coupling limit where κ=1.15.

Nematogen mixtures involving crosslinked polymers with side chain LC exhibit different phase properties not only with regards to the transition temperatures $T_{NI\,1}$, $T_{NI\,2}$, and the coupling parameter κ but also by their isotropic parameters. In particular, the parameters of rubber elasticity α, β, the polymer volume fraction at crosslinking φ_0, the degree of crosslinking described by N_c, and the Flory-Huggins interaction parameter χ are important in determining the phase behavior. This is illustrated in figure 15 which displays the phase diagram using α, β, and χ-parameter functions of composition[38]. The diagram shows that the biphasic regions I+I, N+I, and N+N are reduced to the immediate vicinity of φ_1=1. This is in contrast with figures 13 and 14 where these regions cover a wider range of composition. Another characteristic feature is the emergence of a miscibility gap of the network in the nematic phase.

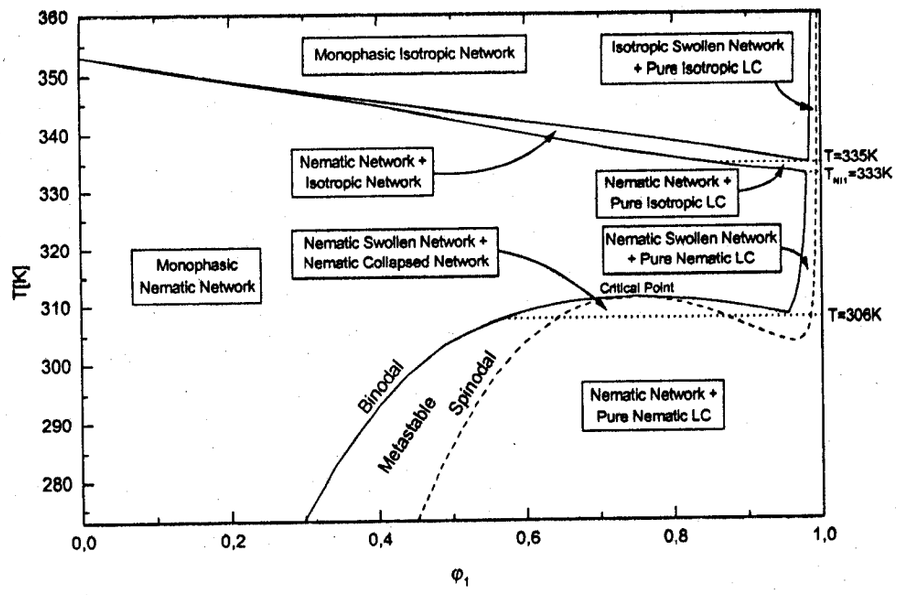

Figure 15

Phase diagram of a binary nematogen mixture composed of a SCLC crosslinked polymer network and a LMWLC. The solid line is the binodal and the dashed line is the spinodal. The phases are indicated on the diagram. The parameters used to plot this figure are

$$\chi = \chi_0 + \chi_1\varphi_2 + \chi_2\varphi_2^2 \qquad ; \chi_0 = -0.35 + \frac{342}{T}; \quad \chi_1 = 0.3; \quad \chi_2 = 0.04$$

$$\alpha = \frac{f-2+2\varphi_2}{f}, \quad \beta = \frac{2\varphi_2}{f}; \; f=3; \; \varphi_0=0.25$$

$N_1=1$; $N_c=10^3$ (loosely crosslinked network); $T_{NI1}=60°C$; $T_{NI2}=80°C$; $\kappa=1$.

A swollen nematic network coexists with a collapsed nematic network. A triple point is found at 33°C where the latter networks are in equilibrium with a pure nematic LC phase. Another triple point is found at 62°C where a nematic network, an isotropic network, and a pure isotropic LC phase coexist. This diagram is obtained for a loosely crosslinked network corresponding to $N_c=1000$. To illustrate the effect of N_c keeping other parameters

constant, we plot in figure 16 the phase diagram corresponding to a highly crosslinked network with N_c=10. Here the miscibility gap within the nematic network does not exist and only one triple point at T=67°C is recovered. The biphasic domain of I+I, N+I, N+N extend to larger ranges of temperature and composition as in figure 15. The higher crosslinking density favors phase separation in the nematic order and in the isotropic state.

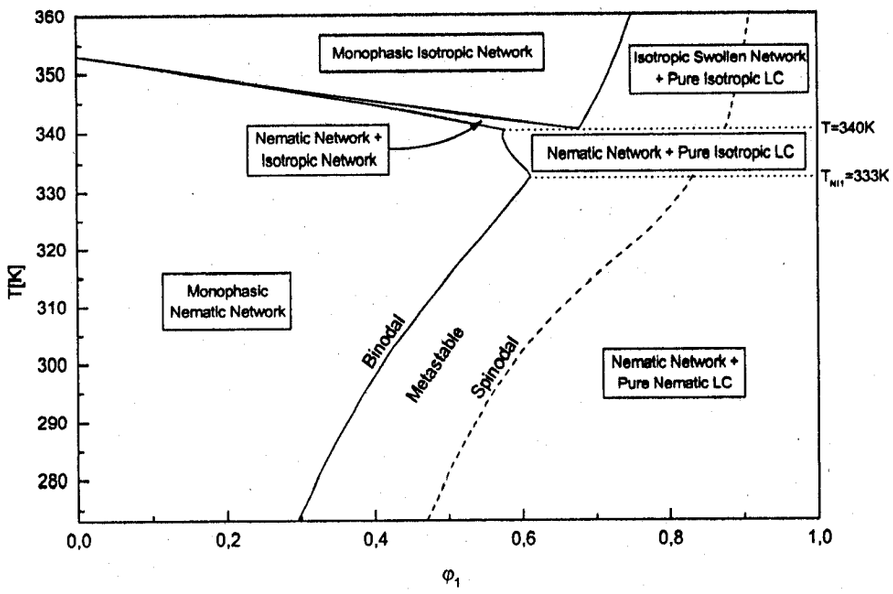

Figure 16

The same parameters as in figure 15 with N_c=10 (highly crosslinked network). The phases in different regions are indicated in the figure.

4. Conclusions

In part 1, phase diagrams of model systems made of mixtures of polymers and LMWLC are reviewed. Several cases are considered to identify the effects of the polymer architecture and the LC order on the phase behavior. A particular attention is given to differentiate between systems involving linear and crosslinked polymers. Systems involving LMWLC with either nematic or smectic-A order were the subject of a particular attention. Phase diagrams of binary nematogens are analyzed underlying the effect of coupling on their miscibility under various conditions. The thermodynamics under the isotropic conditions are described using the Flory-Huggins lattice theory if the polymer is linear and the Flory-Rehner theory of rubber elasticity if the polymer is crosslinked. The presence of crosslinks is shown to have a strong influence upon the phase diagram. In the nematic ordered state, the thermodynamics are described by the Maier-Saupe theory. For mixtures exhibiting a smectic-A order, the extension of the Maier-Saupe theory developed by McMillan is used. For binary nematogens, the phase behavior is described by a free energy model suggested by Brochard et al. and later extended by Kyu et al. to different coupling cases. In spite of their simplicity, these theoretical models are remarkably useful in the interpretation of experimental phase diagrams obtained on various mixtures with linear or crosslinked polymers and various LMWLC showing a nematic or a smectic-A order.

Mixtures of linear poly(n-butylacrylate) of molecular weight near 100 000 g/mol and the nematic LMWLC known as E7 were investigated by polarized optical microscopy (POM) and light scattering (LS)[39]. E7 is an eutectic mixture of four cyanoparaphenylene species. Although its components have different transition temperatures, the E7 mixture is characterized by a single transition temperature T_{NI}=60°C. This is an example of a temperature composition phase diagram obtained from a system made of linear polymer

and a LMWLC mixture which has been analyzed by the present formalism. The data seem to indicate that the eutectic mixture E7 undergoes a phase separation in the presence of polymer probably because of a preferential solubility of some of its constituants with regards to the polymer. A loss of miscibility of the higher molecular weight component of LC with respect to the polymer would lead to a different composition of the LC within ordered domains. Similar observations were made by Nolan et al. on mixtures of UV-cured NOA65 and E7[40]. In this system the nematic-isotropic transition is observed at 65.6°C at the composition of 60wt% LC.

On the other hand, phase diagrams of other mixtures of linear polystyrene (PS) and 8CB were analyzed using differential scanning calorimetry (DSC), POM, and LS[41,42]. These diagrams were constructed for PS samples with molecular weights spanning the range from 4000 to 200000 g/mol and possessing a narrow molecular weight distribution. The LC 8CB is 4-cyano-4'-n-octyl-biphenyl which has a smectic-nematic transition temperature at 33.5°C and a nematic-isotropic transition at 40.5°C. At 21.5°C, it undergoes a transition to a crystalline phase. All the diagrams show an upper critical solution temperature. Because of enhanced compatibility of the low molecular weight polymer and 8CB, neither the critical point nor the I+I miscibility gap was observed. For a high molecular weight polymer, these features were clearly observable and consistent with the mean-field predictions as described in the present theoretical formalism. The smectic-nematic transition takes place approximately at the same temperature for all molecular weights since the LC rich phase is practically pure. A slight tendancy towards a decrease of this transition temperature is seen in the vicinity of the limit of miscibility curve. The diagrams for all systems were successfully analyzed with the theory presented earlier. This was also the case for other systems investigated consisting of high molecular weight polymers and LMWLC with various characteristics[37, 43,44]. Interestingly, although based on mean field

models, the theoretical formalism reviewed here was successful in describing various experimental data with a remarkable accuracy and a good agreement.

References

[1] S. Chandrasekhar, *Liquid Crystals*, 2nd edition, Cambridge University Press, Cambridge 1992

[2] P. G. de Gennes, *The Physics of Liquid Crystals*, Oxford University Press, Ely House, London 1974

[3] J. W. Doane, "Polymer Dispersed Liquid Crystal Displays", in: *Liquid Crystals: Their Applications and Uses*, B. Bahadur, Ed., World Scientific, Singapore 1990

[4] P. S. Drzaic, *Liquid Crystal Dispersions*, World Scientific, Singapore 1995

[5] U. Maschke, X. Coqueret, C. Loucheux, *J. Appl. Polym. Sci.* **56**, 1547 (1995)

[6] U. Maschke, A. Traisnel, J.-D. Turgis, X. Coqueret, *Mol. Cryst. Liq. Cryst.* **299**, 371 (1997)

[7] H. Finkelmann, "Liquid-Crystalline Sidechain Polymers", in : *Polymer Liquid Crystals*, A. Ciferri, W. R. Krigbaum, R. B. Meyer, Eds., Academic Press, New York 1982

[8] P. G. de Gennes, *The Physics of Liquid Crystals*, Oxford University Press, Ely House, London 1974

[9] C. Shen, T. Kyu, *J. Chem. Phys.*, **102**, 556 (1995)

[10] H. W. Chiu, T. Kyu, *J. Chem. Phys.* **103**, 7471 (1995)

[11] F. Brochard, J. Jouffroy, P. Levinson, *J. Phys. (Paris)* **45**, 1125 (1984)

[12] H. M. J. Boots, J. G. Kloosterboer, C. Serbutoviez, F. J. Touwslager, *Macromolecules* **29**, 7683 (1996)

[13] U. Maschke, N. Gogibus, A. Traisnel, X. Coqueret, *Liq. Cryst.* **23**, 457 (1997)

[14] P. J. Flory, *Principles of Polymer Chemistry*, Cornell University Press, Ithaca 1965

[15] M. Warner, X. J. Wang, *Macromolecules* **25**, 445 (1992)

[16] H. Finkelmann, G. Rehage, Adv. Polym. Sci. **60/61**, 100 (1984)

[17] D. Nwabunma, T. Kyu, *Macromolecules* **32**, 664 (1999)

[18] U. Maschke, X. Coqueret, M. Benmouna, *Polym. Networks Blends* **7**, 23 (1997)

[19] F. Benmouna, L. Bedjaoui, U. Maschke, X. Coqueret, M.Benmouna, *Macromol. Theory Simul.* **7**, 599 (1998)

[20] F. Benmouna, X. Coqueret, U. Maschke, M. Benmouna, *Macromolecules* **31**, 4879 (1998)

[21] F. Benmouna, U. Maschke, X. Coqueret, M.Benmouna, *Macromol. Theory Simul.* In press

[22] W. Maier, A. Saupe, *Z. Naturforschung*, **14a**, 882 (1959)

[23] W. Maier, A. Saupe, *Z. Naturforschung*, **15a**, 287 (1960)

[24] W. L. McMillan, *Phys. Rev. A*, **4**, 1238 (1971)

[25] P. J. Flory, J. Rehner, *J. Chem. Phys.*, **12**, 412 (1944)

[26] L. R. G. Treolar, *The physics of Rubber Elasticity*, 3rd edition, Clarendon Press, Oxford 1975

[27] H. James, E. J. Guth, *J. Chem. Phys.* **15**, 669 (1947)

[28] P. J. Flory, *J. Chem. Phys.* **18**, 108 (1950)

[29] Z. S. Petrovic, W. J. MacKnight, R. Koningsveld, K. Dusek, *Macromolecules*, **20**, 1088 (1987)

[30] R. Briber, B. J. Bauer, *Macromolecules* **24**, 1899 (1991)

[31] B. J. Bauer, R. Briber, C. C. Han, *Macromolecules* **22**, 940 (1989)

[32] R. Moerkerke, R. Koningsveld, H. Berghmans, K. Dusek, K. Solc, *Macromolecules* **28**, 1103 (1995)

[33] R. Moerkerke, F. Meeussen, R. Koningsveld, H. Berghmans, W. Mondelaers, E. Schacht, K. Dusek, K. Solc, *Macromolecules* **31**, 2223 (1998)

[34] R. Koningsveld, L. A. Kleintjens, A. R. Shultz, *J. Polym. Sci., Part A2* **8**, 1261 (1970)

[35] H. Arnold, H. Sackmann, *Z. Phys. Chem.* **213**, 137 (1960)

[36] H. Arnold, H. Sackmann, *Z. Phys. Chem.* **213**, 145 (1960)

[37] F. Benmouna, B. Pen, J. Rühe, D. Johannsmann, *Liquid Crystals*, In press

[38] F. Benmouna, U. Maschke, X. Coqueret, M.Benmouna, *J. Polym. Sci. Part B : Polym. Phys. Ed.* submitted

[39] T. Bouchaour, F. Benmouna, L. Leclercq, B. Ewen, X. Coqueret, M. Benmouna, U. Maschke, *Liquid Crystals*, submitted

[40] P. Nolan, M. Tillin, D. Coates, *Mol. Cryst. Liq. Cryst. Lett.* **8**, 129 (1992)

[41] F. Benmouna, A. Daoudi, F. Roussel, J.-M. Buisine, X. Coqueret, U. Maschke, *J. Polym. Sci. Part B : Polym. Phys. Ed.* **37**, 1841 (1999)

[42] F. Benmouna, A. Daoudi, F. Roussel, J.-M. Buisine, X. Coqueret, U. Maschke, *Macromolecules*, submitted

[43] H. W. Chiu, Z. L. Zhou, T. Kyu, L. G. Cada, L.-C. Chien, *Macromolecules* **29**, 1051 (1996)

[44] M.-C. Chang, H.-W. Chiu, X.Y. Wang, T. Kyu, N. Leroux, S. Campbell, L.-C. Chien, *Liquid Crystals* **25**, 733 (1998)

PART 2

Effect of molecular weight on the phase diagram and thermal properties of poly(styrene)/8CB mixtures

Abstract

Equilibrium phase diagrams and thermophysical properties of mixtures of poly(styrene) (PS) and 4-cyano-4'-*n*-octyl-biphenyl (8CB) are investigated. Three systems with widely different molecular weights of the polymer are considered in an attempt to assess the effects of the polymer size on the miscibility of PS and 8CB. The experimental phase diagrams are established using polarized optical microscopy (POM), light scattering (LS), and differential scanning calorimetry (DSC) and the results analyzed with the predictions of the Flory-Huggins theory of isotropic mixing and the Maier-Saupe theory of nematic order generalized by McMillan to include smectic-A order. Good agreement is observed between theory and experiments. The solubility properties of mixtures with different polymer sizes are analyzed using the method suggested by Smith. The solubility limit of 8CB in PS is deduced from enthalpy changes at the nematic-isotropic transition temperature (T_{NI}) as a function of polymer molecular weight. It is found that the decrease of the solubility limit with increasing molecular weight is not linear and reaches a plateau value for higher molecular weights. The results obtained for the systems investigated here and for three other systems reported in the literature fall on a single master curve representing the solubility limit at T_{NI} as a function of polymer molecular weight.

1. Introduction

This part deals with the equilibrium phase behavior and the thermo-physical properties of mixtures of polystyrene (PS) and a low molecular weight liquid crystal (LMWLC) (4-cyano-4'-*n*-octyl-biphenyl or 8CB). Samples made of linear flexible chains with no mesogen groups and three different molecular weights dissolved in a low molecular weight LC are considered. This allows one to assess the effects of polymer size on the equilibrium phase behavior and thermal properties of polymer/LC mixtures. The LC 8CB exhibits in the bulk three distinct transitions and presents crystalline, smectic-A and nematic phases. Mixtures covering a wide range of compositions were prepared following the same procedure based on a combination of solvent induced phase separation (SIPS) and thermally induced phase separation (TIPS).[1-2] Equilibrium phase behavior and thermophysical properties of these systems are the subject of a growing interest because of the key role they play in a variety of practical applications such as digital displays, privacy windows, computers, TV screens etc.[1-4] Developing reliable methods to evaluate the content of LC dissolved in the polymer with a high accuracy is crucial for determining the optimal operating conditions of devices made of such systems. It is clear that reduction of the amount of LC dissolved in the polymer matrix is not only an economic incentive to reduce cost of these devices but also a goal sought to improve their operating conditions.[5-6] With regards to the thermophysical properties, the LC dissolved in the polymer acts generally as a plasticizer reducing its glass transition temperature.[7,8] Moreover, it affects strongly the refractive index matching condition between the polymer and the component of the LC perpendicular to its director. This condition is required to achieve maximum transmission of light when an electric field is applied.[9-11]

In the present work we have choosen a model system made of well characterized PS and a single component LMWLC with well defined transition temperatures including smectic A-

nematic and nematic - isotropic transitions. Three PS samples covering a wide range of molecular weight and a very narrow molecular weight distribution were used. Under such conditions we were able to characterize unambiguously the effect of polymer molecular weight on the phase diagram. To our knowledge similar experimental investigation was only reported by Kyu et al. who considered blends of polymethylmethacrylate and the eutectic LMWLC mixture known as E7 with a nematic - isotropic transition temperature of 60°C.[12] The phase diagram and the phase separation dynamics of PS (M_w=218000 g/mol)/ E7 has been investigated by Kim and Kyu.[13]

In a recent paper,[14] preliminary data obtained by polarized optical microscopy (POM) and differential scanning calorimetry (DSC) of PS/8CB were given. These data were taken on a PS/8CB mixture where the polymer had a fixed molecular weight M_w=44·10^{3}g/mol with a narrow distribution corresponding to M_w/M_n=1.05. The experimental phase diagram was reported and some thermophysical properties such as the glass transition temperature T_g and the fraction of LC in the nematic domains α were briefly described.

The present paper is an extension of the preceeding one in several ways. First, two additional systems characterized by molecular weights of PS differing by orders of magnitude are considered. This allows one to assess unambigously the effects of the polymer size on the equilibrium phase diagram and thermal properties of PS/8CB blends. By choosing widely different sizes, one hopes to reach conclusions representative of the whole range of polymer molecular weights from 4·10^3 to 200·10^3 g/mol. Unlike reference 14, the experimental data obtained here by POM, LS, and DSC are analyzed in more detail using a theoretical model which combines the Flory-Huggins[15] theory for isotropic mixing and the Maier-Saupe[16,17] theory for nematic order supplemented by the McMillan[18] extension to include the effects of smectic-A order. Changes in thermophysical properties resulting from changes in the polymer size are also considered. Enthalpy changes at the

nematic-isotropic transition with LC composition yield valuable information on the solubility parameters and the amount of LC remaining in the polymer after the phase separation. New predictions on the solubility limit of the LC in different systems are made as a function of polymer molecular weight.

2. The theoretical phase diagram

The theoretical formalism which describes the phase behavior of mixtures of linear polymers and LMWLCs with smectic - nematic and nematic - isotropic transitions can be found in the literature.[19-27] A summary of this formalism is given in the present section. Valuable information is gained in the analyzis of experimental data with regards to the effects of polymer size, transition temperatures, combined isotropic and anisotropic interactions etc. The general equations are given first before the explicite forms of free energies and chemical potentials, and the procedure by which the equilibrium phase diagram is constructed.

a) General equations

The starting free energy density for the systems under consideration here is a sum of two terms

$$f = f^{(i)} + f^{(a)} \tag{1}$$

The letter f represents a free energy density and the superscripts (i) and (a) stand for isotropic and anisotropic, respectively. For the entire system containing a total number of N_t molecules, the total free energy is $F=N_t f$ with $N_t=N_1 n_1+N_2 n_2$; N_k and n_k being the degree of polymerization and the number of molecules per unit volume of species k, respectively, with k=1 for the LC and k=2 for the polymer. Similarly, we have $F^{(i)}=N_t f^{(i)}$ and $F^{(a)}=N_t f^{(a)}$. Knowledge of the free energy allows the calculation of the chemical potentials

which in turn are used to determine the composition of phases in equilibrium. These are given by the derivatives

$$\mu_1 = \left(\frac{\partial F}{\partial n_1}\right)_{n_2,T,P} \quad ; \quad \mu_2 = \left(\frac{\partial F}{\partial n_2}\right)_{n_1,T,P} \tag{2}$$

where P and T represent pressure and temperature, respectively, and the quantities in the subscripts remain constant in the derivation. Sometimes it is more convenient to write the chemical potentials in terms of derivatives with respect to volume fractions $\varphi_1=n_1N_1/N_t$ and $\varphi_2 =n_2N_2/N_t$. It will be assumed that all segments occupy the same volume and the mixture is incompressible implying $\varphi_2=1-\varphi_1$. One finds

$$\frac{\mu_1}{N_1} = f - \varphi_2 \frac{\partial f}{\partial \varphi_2} \tag{3}$$

$$\frac{\mu_2}{N_2} = f - \varphi_1 \frac{\partial f}{\partial \varphi_1} \tag{4}$$

If two phases designated by single and double primes are in equilibrium, their compositions are given by the standard equations

$$\mu_1^{(')} = \mu_1^{(")} ; \quad \mu_2^{(')} = \mu_2^{(")} \tag{5}$$

which are written explicitly as follows

$$f - \varphi_1 \left.\frac{\partial f}{\partial \varphi_1}\right|^{(')} = f - \varphi_1 \left.\frac{\partial f}{\partial \varphi_1}\right|^{(")} \tag{6}$$

$$\left.\frac{\partial f}{\partial \varphi_1}\right|^{(')} = \left.\frac{\partial f}{\partial \varphi_1}\right|^{(")} \tag{7}$$

The same relationships hold for isotropic, anisotropic and total free energies. The choice of any of these contributions depends on the nature of phases in equilibrium. These general formulae are useful in the construction of the phase diagram. Their application to the systems under consideration here is based on a combination of the Flory-Huggins theory of

isotropic mixing and the Maier-Saupe-McMillan theory of nematic and smectic orders as we will discuss in the following sections.

b) The Flory-Huggins theory of isotropic mixing

The Flory-Huggins free energy density for a binary mixture is well known

$$\frac{f^{(i)}}{k_B T} = \frac{\varphi_1}{N_1}\ln\varphi_1 + \frac{\varphi_2}{N_2}\ln\varphi_2 + \chi\varphi_1\varphi_2 \tag{8}$$

where k_B is the Boltzman constant and χ the Flory-Huggins interaction parameter. Substituting eq 8 into eqs 3 and 4 yields

$$\frac{\mu_1^{(i)}}{k_B T} = \ln\varphi_1 + \left(1 - \frac{N_1}{N_2}\right)\varphi_2 + \chi N_1 \varphi_2^2 \tag{9}$$

$$\frac{\mu_2^{(i)}}{k_B T} = \ln\varphi_2 + \left(1 - \frac{N_2}{N_1}\right)\varphi_1 + \chi N_2 \varphi_1^2 \tag{10}$$

Likewise, the derivation of the isotropic free energy with respect to φ_1 is straightforward. Assuming that χ is independent of composition yields

$$\frac{\partial f^{(i)}}{\partial \varphi_1} = \frac{\ln\varphi_1 + 1}{N_1} - \frac{\ln\varphi_2 + 1}{N_2} + \chi(\varphi_2 - \varphi_1) \tag{11}$$

These results are sufficient to describe the isotropic phase behavior of the mixture. One needs only to specify the variation of χ with temperature. The following form is adopted here

$$\chi = A + \frac{B}{T} \tag{12}$$

where A and B are constant independent of T. They are chosen to obtain the best fit with the experimental data in the part of the diagram where the isotropic interaction is most significant.

c) The Maier-Saupe-McMillan theory of nematic and smectic-A orders

The anisotropic free energy is obtained from the Maier-Saupe theory of nematic order generalized by McMillan to include smectic-A order.[19-27] Therefore, two order parameters are needed: the nematic order parameter s describes the orientation distribution defined by the angle θ between the LC director and a reference axis 0z

$$s = \frac{1}{2}\left[3\langle cos^2\theta\rangle - 1\right] \tag{13}$$

The smectic-A order parameter σ describes ordering along the 0z-direction

$$\sigma = \frac{1}{2}\left\langle\left(3\cos^2\theta - 1\right)\cos\frac{2\pi z}{d}\right\rangle \tag{14}$$

The symbols <--> denote averages with respect to the distribution of angle θ and coordinate z (along the direction of the smectic order), d is the distance between consecutive smectic layers. The function $g(z, \mu)$ represents the distribution of director orientations

$$g(z,\mu) = \frac{\exp\left[-(u_n + u_s)/k_B T\right]}{4\pi Z} \tag{15}$$

where $\mu = \cos\theta$; u_n and u_s are the mean field potentials for nematic and smectic interactions. They are expressed in terms of mean field parameters m_n and m_s as follows

$$\frac{u_n}{k_B T} = -\frac{m_n}{2}(3\mu^2 - 1) \tag{16}$$

$$\frac{u_s}{k_B T} = -\frac{m_s}{2}(3\mu^2 - 1)cos^2\frac{2\pi z}{d} \tag{17}$$

The capital letter Z represents the partition function and is related with the nematic and smectic orders

$$Z = \iint d\mu dz \exp\left[\frac{m_n}{2}(3\mu^2 - 1)\right]\exp\left[\frac{m_s}{2}(3\mu^2 - 1)\cos 2\pi\frac{z}{d}\right] \tag{18}$$

The anisotropic free energy is given in terms of the distribution function

$$\frac{f^{(a)}}{k_B T} = \frac{F^{(a)}}{n_0 k_B T} = \frac{\varphi_1}{N_1}\left\{\iint g(z,\mu)\ln[4\pi g(z,\mu)]d\mu dz - \frac{1}{2}\nu\varphi_1\left(s^2 + \alpha\sigma^2\right)\right\} \quad (19)$$

The first term on the right hand side of eq 19 is the entropy cost due to nematic/smectic orders while the second term is an energy contribution. The integral defining the entropy can be reduced as

$$\iint d\mu dz\; g(z,\mu)\ln[4\pi\; g(z,\mu)] = \ln Z - m_n s - m_s\sigma \quad (20)$$

Minimization of the free energy with respect to the two order parameters (i.e. $\frac{\partial f^{(a)}}{\partial s} = 0$ and $\frac{\partial f^{(a)}}{\partial \sigma} = 0$ yields the mean field parameters m_n and m_s in terms of the order parameters s and σ

$$m_n = \nu\, s\, \varphi_1; \quad m_s = \zeta\, \nu\, \sigma\, \varphi_1 \quad (21)$$

Combining eqs 19 to 21 yield the anisotropic free energy

$$\frac{f^{(a)}}{k_B T} = \frac{\varphi_1}{N_1}\left[-\ln Z + \frac{1}{2}\nu\varphi_1(s^2 + \zeta\sigma^2)\right] \quad (22)$$

where ν represents the quadrupole interaction parameter in the Maier-Saupe theory and ζ the strength of smectic interaction in the McMillan model. The former is given by ν=4.54T_{NI}/T while ζ depends upon the ratio T_{SN}/T_{NI}. According to the theory of McMillan, and for the system under consideration here where T_{SN}/T_{NI}=0.98, the parameter ζ will be given the value ζ=0.9375.

The anisotropic chemical potentials are obtained by a straigthforward derivation of eq 22 using eqs 3 and 4. The results are

$$\frac{\mu_1^{(a)}}{k_B T} = -\ln Z + \frac{1}{2}\left(s^2 + \zeta\sigma^2\right)\nu\varphi_1^2 \quad (23)$$

$$\frac{\mu_2^{(a)}}{k_B T} = \frac{1}{2}\frac{N_2}{N_1}\left(s^2 + \zeta\sigma^2\right)\nu\varphi_1^2 \quad (24)$$

The above formalism is sufficient to construct the theoretical phase diagrams by a proper choice of the parameters characterizing the PS/8CB mixtures as we shall see in the following sections of this paper.

3. Experimental part

a) Sample description

PS samples of different molecular weights were purchased from Aldrich (Saint Quentin Fallavier, France) and were used without purification. The molecular weights and their distributions were obtained by GPC calibrated with standard PS samples. These measurements were performed in tetrahydrofuran (THF) at room temperature and led to a) M_w=4·10^3 g/mol, M_w/M_n=1.06 ; b) M_w=44·10^3 g/mol, M_w/M_n=1.05 ; c) M_w=200·10^3 g/mol, M_w/M_n=1.09.

The LC is 4-cyano-4'-*n*-octyl-biphenyl or 8CB showing a smectic-A order. It was purchased from Frinton Laboratories (New Jersey, USA) and presents in the pure state characteristic transition temperatures which were provided by the manufacturer as : T_{KS} = 21.5°C, T_{SN} = 33.5°C, and T_{NI} = 40.5°C.

b) Sample preparation

PS and 8CB with different LC compositions were dissolved in THF at 50 wt% (weight fraction). Mixtures were stirred mechanically for 12 hours. Samples were prepared following the standard procedure for microscopy observations. A small amount of the mixture was cast on a clean glass slide and the sample was left for 24 hours to allow for a complete evaporation of the solvent. Another glass slide was put on top of the first one and the dry sample was sandwiched between the two glass slides. The same procedure is repeated to have two or more samples at the same composition prepared independently to check for reproducibility of the results. Samples with the pure components were also

obtained following a similar procedure and it is worthnoting that the same results were obtained as in the case of the pure components prepared without use of an organic solvent. For the DSC measurements, the samples were prepared by introducing approximately 3mg of the initial mixture into aluminum DSC pans prior to solvent evaporation.

c) DSC measurements

DSC measurements were performed on an apparatus of the type SEIKO DSC 220C equipped with a liquid nitrogen system and allows for cooling and heating ramps. The apparatus cell was purged with nitrogen at a rate of 50ml/min. The same heating-cooling ramps were used for the microscopy measurements in the temperature range spanning from 20°C to 70°C. Data were recorded systematically on the second heating ramp.

Enthalpy changes at the nematic–isotropic transition denoted ΔH_{NI} and in the smectic–nematic transition denoted ΔH_{SN} are given in Joule per gram of the sample. Uncertainties in these measurements were approximately ±0.05 J/g.

d) POM measurements

The polarized optical microscope (POM) used in this study is of type Leica DMRXP, equipped with a heating-cooling stage Linkam THMSE 600. Samples were heated at the rate 2°C/min from room temperature to 15 degrees above the transition temperature leading to the isotropic phase. Then samples were left approximately 5 min in the isotropic state. Afterwards, the samples corresponding to 50 wt% 8CB or higher were cooled down to room temperature at a rate of -2°C/min. For the other samples with low concentration in LC, cooling was performed to T=-10°C to allow for phase separation and formation of ordered regions if a LC phase does exist. This procedure is followed after 5 min by a heating ramp at a rate of 2°C/min. Transition temperatures were recorded during the heating ramp.

e) LS measurements

Light scattering measurements were performed using the classical setup illustrated in Figure 1 of reference[28]. The He-Ne Laser (λ=632.8 nm) was polarized linearly, perpendicular to the scattering plane. The scattered intensity was measured in the VV mode (I_{vv}), where the analyser axis is parallel to the polarization direction of the incident beam. The scattering pattern was recorded by a CCD camera. No anisotropic effects were found on the intensity pattern allowing to perform radial averages of the scattered intensity. The samples already used for POM measurements were submitted to the same heating/cooling cycle as described in the previous section. In the isotropic state at temperatures above 70°C, the scattering intensity was constant exhibiting low values. The temperature at which the scattering intensity undergoes a sharp or discontinuous increase was taken as the onset of phase separation.

4. Results and discussions

4.1. Order parameters and phase diagrams

a) Order parameters

Prior to the discussion of the phase diagrams, it would be useful to understand first the dependence of the order parameters on temperature and composition. The relative contribution of the anisotropic free energy to the total free energy and hence the existence of ordered domains in the phase diagram are related to the values of the order parameters. In view of the importance of these quantities, we represent in Figure 1 the variation of s and σ as a function of φ_1 for three temperatures. Thick and dashed curves represent s and σ, respectively. s undergoes two discontinuities at φ_{SN} and φ_{NI} and exhibits two branches. The anisotropic free energy is nonzero only if the parameters s and σ are higher than the

limiting values s_c and σ_c. Above the smectic-nematic transition temperature (T_{SN}=33.5°C) and below the volume fraction $\varphi_{SN}=T/T_{SN}$, there is no smectic order and σ is zero.

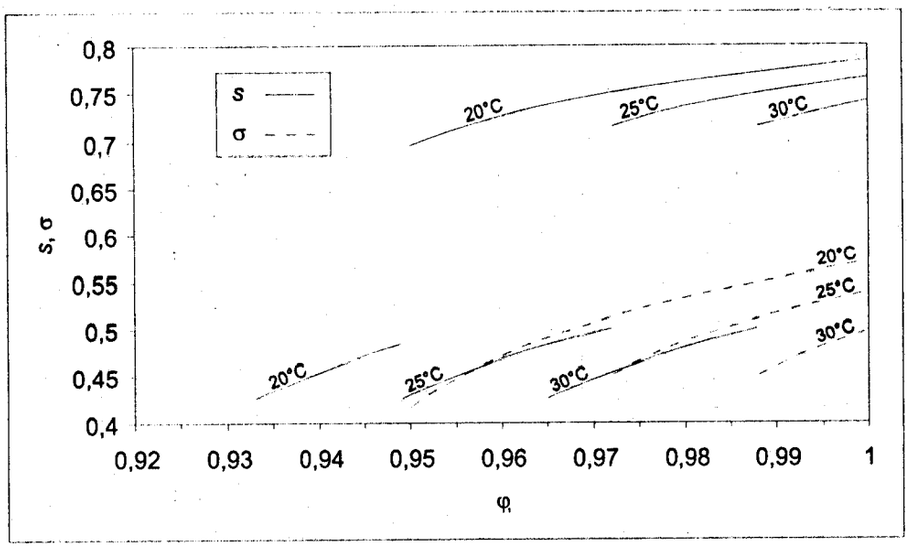

Figure 1

Variations of nematic s and smectic σ order parameters versus LC composition at three temperatures. The following quantities were used in this plot: T_{SN}=33.5°C, T_{NI}=40.5°C, ζ=0.9375.

Above the nematic isotropic-transition temperature (T_{NI}=40.5°C) and below $\varphi_{NI}=T/T_{NI}$ there is no nematic order. Below this composition, the smectic order disappears since σ becomes 0 and the nematic order remains alone until the composition reaches the composition φ_{NI}. The upper branch of the nematic order parameter is quite high due to the enhanced nematic order resulting from the emergence of the smectic-A order. The increase of the order parameter s in the presence of smectic interactions depends upon the coupling parameter α which in turn is function of the ratio T_{SN}/T_{NI}. For the present PS/8CB system, considering the values of T_{NI} and T_{SN} characterizing 8CB we have obtained the value of ζ=0.9375 according to the theory of McMillan.[18] Needless to say that at temperatures

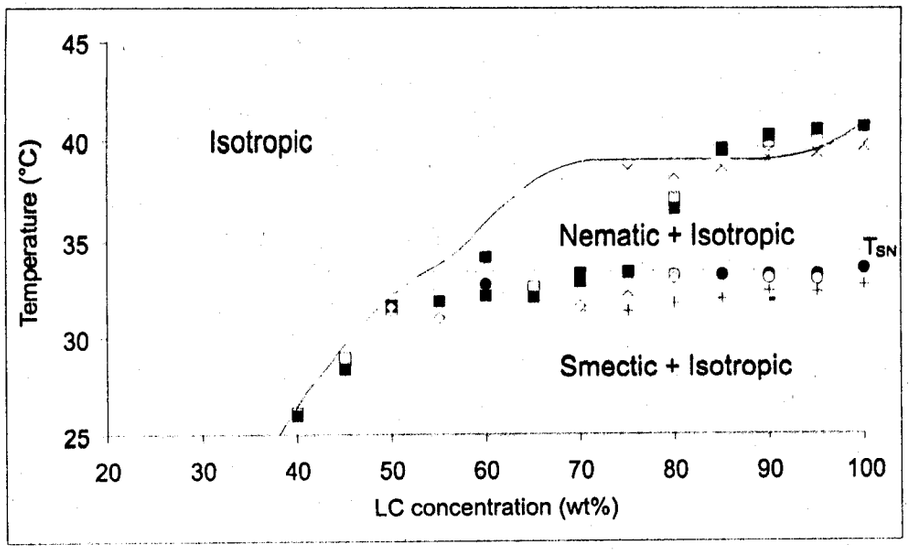

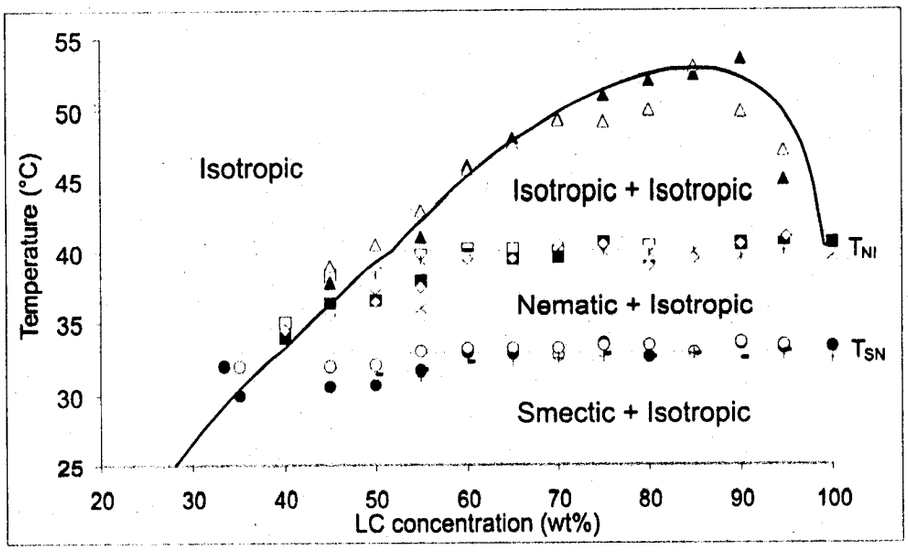

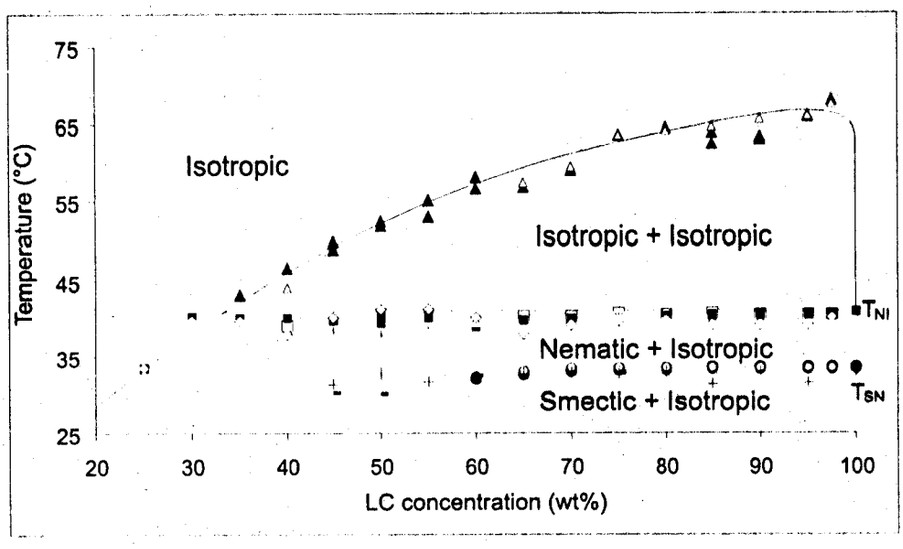

Figure 2 (Caption see next page)

Figure caption to Figure 2 :

Equilibrium phase diagrams of PS / 8CB. The symbols in this diagram represent experimental data obtained by POM and DSC : ○ and ● represent the transition temperature from smectic A + isotropic to nematic + isotropic for the two series of samples by POM measurements; □ and ■ represent the transition temperature from nematic + isotropic to isotropic + isotropic for the two series of samples by POM measurements; Δ and ▲ represent the transition temperature from isotropic + isotropic to isotropic for the two series of samples by POM measurements; + and - represent the transition temperature from smectic A + isotropic to nematic + isotropic for the two series of samples by DSC measurements; x and * represent the transition temperature from nematic + isotropic to isotropic + isotropic for the two series of samples by DSC measurements; 7 represent the transition temperature from nematic + isotropic to isotropic + isotropic or isotropic obtained by LS measurements.

a) $M_w=4\cdot10^3$ g/mol b) $M_w=44\cdot10^3$ g/mol c) $M_w=200\cdot10^3$ g/mol

The solid curves represent the theoretical predictions obtained using the following parameters T_{SN}=33.5°C, T_{NI}=40.5°C, ζ=0.9375, and

a) $\chi=-0.93+531.3/T$; $N_2=15$

b) $\chi=-2.408+1010.76/T$; $N_2=32$

c) $\chi=-4.558+1733.14/T$; $N_2=361$

above T_{SN}=33.5°C only the nematic order survives and the curves display only the lower branch of the solid line.

The results of these calculations together with the theoretical formalism described in section 2 lead to the solid lines in the phase diagrams given below.

b) Phase diagrams

Figure 2a, 2b and 2c show the phase diagrams for the three systems under investigation with M_w=4·10^3, 44·10^3 and 200·10^3 g/mol, respectively. Each of the three phase diagrams were established on the basis of data recorded on two independently prepared samples with practically the same composition. This enables one to double check the validity of the measured data. The symbols represent the experimental results as indicated on the figure captions and the solid lines are the theoretical predictions. The parameters used to plot these lines are chosen to reach the best fit to data. The three diagrams show an upper critical solution temperature shape. Unlike Figure 2a, the other two have a distinct critical point and an (I+I) biphasic region. The temperature and composition at the critical point increase with the molecular weight according to the mean field theory prediction. The number of adjusted parameters to fit experimental data is reduced in the presence of the critical point since the number of repeat units of the polymer N_2 is calculated from the critical volume fraction for each of the two highest molecular weight systems using $\varphi_c=N_2^{1/2}/[N_1^{1/2}+N_2^{1/2}]$ assuming that N_1=1. These values are given in the figure caption. Knowing N_1 and N_2, one can determine the critical interaction parameter using $\chi_c=[N_1^{-1/2}+N_2^{-1/2}]^2/2$. Only one parameter remains to fit the data. Therefore, values are given to A while B is deduced according to $B=[\chi_c-A]T_c$. This procedure was possible in Figures 2b and 2c while in Figure 2a the absence of the critical point makes the choice of fitting parameters more arbitrary. Nevertheless, good agreement is reached between the three sets of experimental data obtained from POM, LS, and DSC, and theoretical predictions. The variations of the χ-parameter with temperature for the three systems chosen to plot the theoretical curves are given in the figure caption.

The diagrams exhibit several regions with a distinct difference between the lowest polymer molecular weight (Figure 2a) and the other two (Figures 2b and 2c). Mixtures with the

short polymer chain do not exhibit the biphasic region of coexisting isotropic phases as in the other cases. This is due to the higher compatibility between the short polymer and the LC as compared to the long polymers. The enhanced compatibility results into a direct transition from the (N+I) region to the homogeneous isotropic phase as soon as the temperature of nematic-isotropic transition is crossed. The system with highest M_w presents the largest miscibility gap which covers a range of temperature up to the critical temperature 65°C, and a domain of composition from approximately 15 to 100 wt% LC as shown in Figure 2c. The transition from smectic to nematic order is observed for the three systems at approximately the same temperature. There is a tendency towards a decrease of this transition appearing for lower LC compositions. This perturbation is probably due to the influence of T_g which is quite close to this region. Apart from this effect, the temperature at which the transition from (S+I) to (N+I) takes place is independent of the molecular weight and is the same as for pure 8CB, namely T_{SN}=33.5°C. This can be easily understood by noting that in the regions (S+I) and (N+I), a polymer rich phase dissolving the LC in the isotropic state is in equilibrium with almost pure LC phase either in the smectic order (lower region S+I) or in the nematic order (upper region N+I). Hence, it is reasonable to expect that the transition temperature from S- to N-order of the LC remains practically constant at 33°C characterizing pure 8CB regardless of the amount of polymer in the sample provided that this amount is sufficient to form an ordered phase. Melting down of the nematic order into an isotropic phase takes place roughly at 40.5°C characteristic of the (N-I) transition of the pure LC for the three systems investigated here. The explanation is the same as above in the transition from smectic to nematic order.

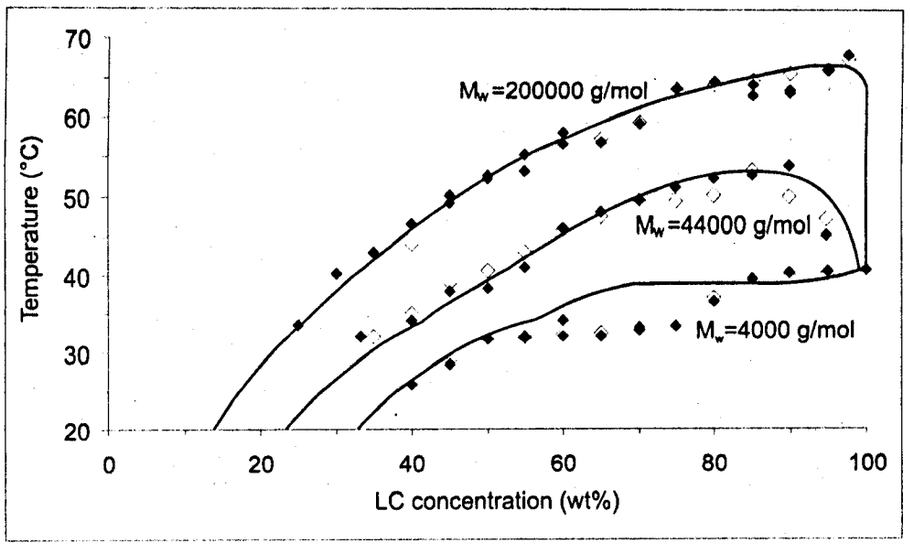

Figure 3

Transition temperatures to the isotropic phase for the three systems in the descending order from the top : $M_w=200\cdot10^3$ g/mol, $M_w=44\cdot10^3$ g/mol, $M_w=4\cdot10^3$ g/mol. The symbols 7 and ◆ represent experimental data obtained by POM, LS, and DSC and the solid lines are theoretical predictions calculated with the parameters given in the caption of Figure 2.

To illustrate further the effect of polymer size on the phase behavior of the three systems, we reproduce in Figure 3, the change in the highest transition temperature with composition only. The upper curve represents the highest molecular weight and shows a transition from an (I+I) to an I region whereas for the lower curve corresponding to the lowest M_w one has a direct transition from an (N+I) region to a single isotropic phase. A drastic loss of miscibility follows an increase of polymer size. Consequently, the amount of LC dissolved in the polymer matrix decreases substantially. Quantification of these tendencies has an important impact upon quality of these systems in practical applications. They represent valuable guides for the choice of adequate materials suitable for some applications.

Optical micrographs showing coexisting domains of smectic-A order with isotropic phases and nematic domains with isotropic phases were given in reference 14 for the system with intermediate molecular weight of PS. Similar textures were obtained for the other systems with minor differences. For example, the ordered domains observed in the system with lowest M_w are less developped and more difficult to identify due to the higher compatibility of the LC and the polymer. The higher molecular weight polymer systems exhibit much larger and more defined ordered domains.

In order to improve understanding of the thermal properties of these systems, it is useful to analyze with further details the energetic data obtained by DSC measurements which is the subject of the following section.

4.2. Thermophysical properties

a) DSC data

Figures 4a and 4b display the thermograms corresponding to mixtures with PS molecular weight M_w=4·10^3 and 200·10^3 g/mol, respectively, and LC composition from 45 to 95 wt% 8CB. The thermograms for M_w=44·10^3 g/mol were given in reference 14 and are not reproduced here. Measurements made for the system with M_w=44·10^3 g/mol up to 30 wt% 8CB revealed a plasticizing effect of the LC for PS via a sharp decrease of the glass transition temperature T_g from 103°C for pure PS down to about 17°C for 30 wt% LC. For this system, up to 30 wt% 8CB, there is complete miscibility of PS and 8CB. The DSC thermograms exhibit a single glass transition and the sample remains isotropic at all temperatures covered in the experiments. For the PS of highest molecular weight, the range of miscibility shrinks substantially, and a gap appears at less than 15 wt% 8CB for T=20°C for example.

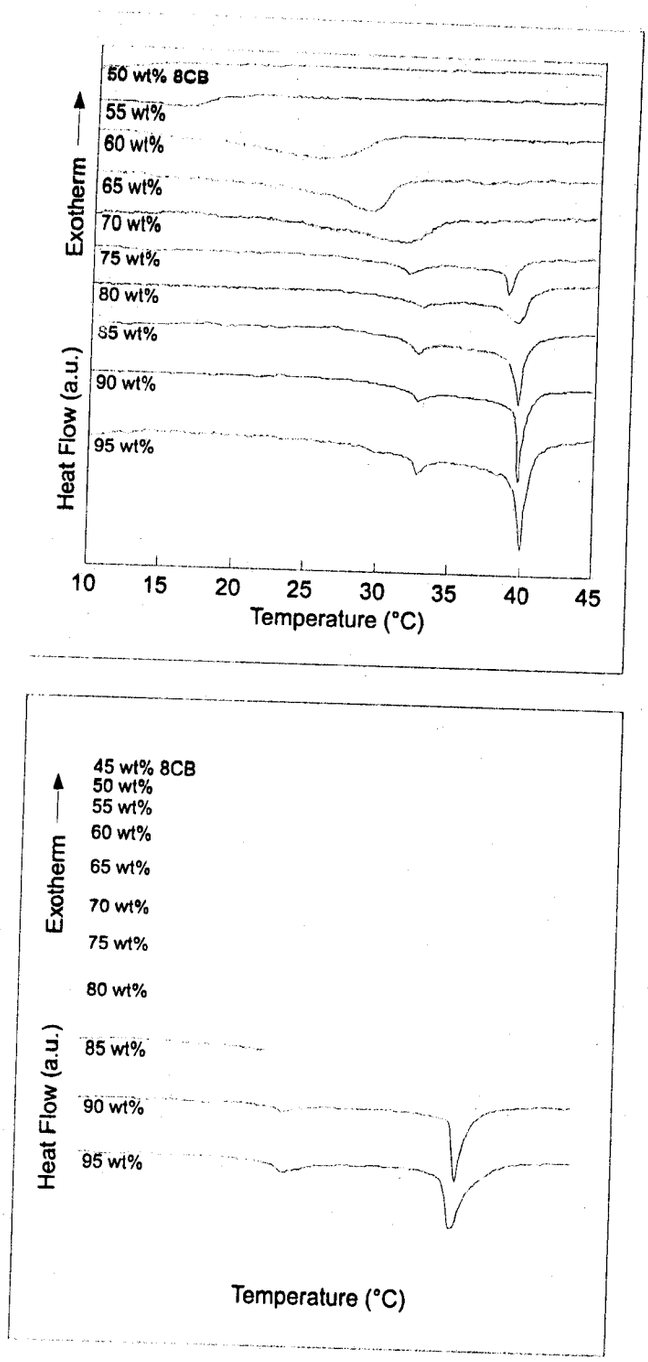

Figure 4

a- DSC thermograms of the PS/8CB mixture with M_w=4·10^3 g/mol of compositions from 50 to 95 wt% 8CB recorded during the second heating at a rate of 2°C/min.

b- The same as in a) for M_w=200·10^3 g/mol recorded under similar conditions in a composition range from 45 to 95wt% 8CB.

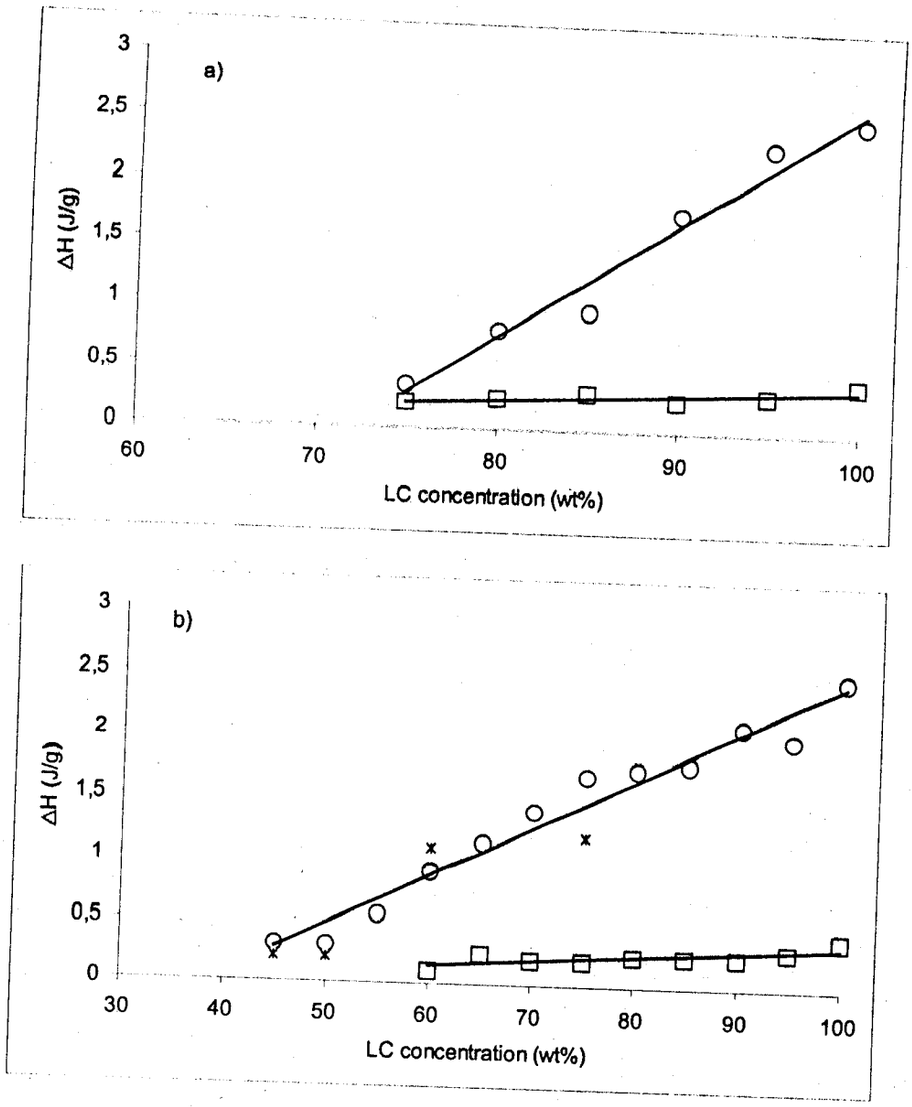

Figure 5

Enthalpy variations in the nematic-isotropic transition ΔH_{NI} and the smectic A - nematic transition ΔH_{SN} versus 8CB concentration.

a) $M_w=4\cdot10^3$g/mol

b) $M_w=200\cdot10^3$g/mol

x correspond to data obtained independently from a second series of samples of $M_w=200\cdot10^3$g/mol. The symbol □ represents data of ΔH_{SN}.

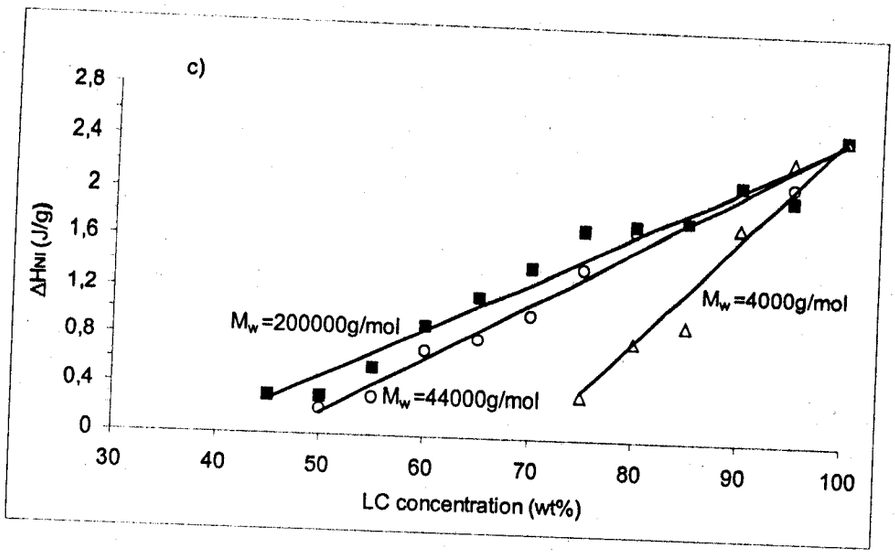

Figure 5

c) Only ΔH_{NI} versus LC concentration for the three molecular weights.

The symbols ■, ○ and Δ represent the ΔH_{NI} data for the three systems in the descending order of M_w.

b) Enthalpy data

Figure 5a and 5b represent enthalpy changes at the (S+N) and (N+I) transitions versus composition for the mixtures with lowest and highest molecular weights, respectively. Enthalpy changes in the (N+I) transition are larger that in the (S+N) transition. The energy cost to align randomly oriented LC molecules to form a nematic phase is much higher than to rearrange the oriented molecules and achieve a smectic-A order. This is true for the three systems considered here. The results for the intermediate molecular weight are not reproduced here and can be found in reference 14. Measurements of enthalpy changes in the (N+I) transition are much more precise than the (S+N) transition which shows scattered data. Observations made from the ΔH_{NI} data are more reliable and therefore we shall proceed with the discussion of thermophysical properties extracted from the (N+I) energy data only.

In order to allow comparison of the results obtained for different molecular weights, we present in Figure 5c ΔH_{NI} versus $\varphi_{LC}= \varphi_I$ for the three systems investigated. One observes that ΔH_{NI} increases linearly with LC content and the three curves merge together at $\varphi_I=1$ to the same value 2.6 J/g. The increase of ΔH_{NI} is steeper for lower molecular weight as the concentration of LC increases.

c) Solubility data

The above thermal data enable one to extract the solubility limit β of the LC in the polymer which gives a direct estimate of the relative amount of LC in nematic domains. Let δ be the ratio of enthalpy changes at the (N+I) transition for the mixture at composition φ_I and for the bulk LC

$$\delta = \Delta H_{NI}(\varphi_I) / \Delta H_{NI}(\varphi_I=1) \tag{25}$$

The rule of inverse segments yields a relationship between δ and the solubility limit β as

$$\delta = (\varphi_I-\beta) / (1-\beta) \tag{26}$$

where $\varphi_I>\beta$, otherwise $\delta=0$. This assumes that the LC inside nematic domains and in the pure state have similar thermophysical properties and that the polymer dissolved in the LC phase does not contribute to the enthalpy change $\Delta H_{NI}(\varphi_I)$. Moreover, the (N+I) transition temperature is assumed to remain constant upon addition of polymer.

Figure 5c shows that $\Delta H_{NI}(\varphi_I)$ increases linearly with φ_I consistent with Eq 26 and literature data.[5,6,8,9,29,30] The intercepts of the lines with the x-axis yield the solubility limit β and decreases strongly with increasing molecular weight of the polymer. One reads β=0.37,0.47 and 0.71 in the decreasing order of PS molecular weight. It is interesting to note that for the systems investigated by Smith[5] which usually involve chemically cross-linked networks, the typical values of β vary from 0.1 to 0.2. In view of these remarks, we see that the present values of β are comparatively high. On the other hand, the fraction of

8CB contained in the nematic domain α is another interesting quantity. It is given by the ratio of the mass of LC in the nematic domain m_1^D and that of the LC in the whole mixture m_1

$$\alpha = m_1^D / m_1 = \delta / \varphi_1 \tag{27}$$

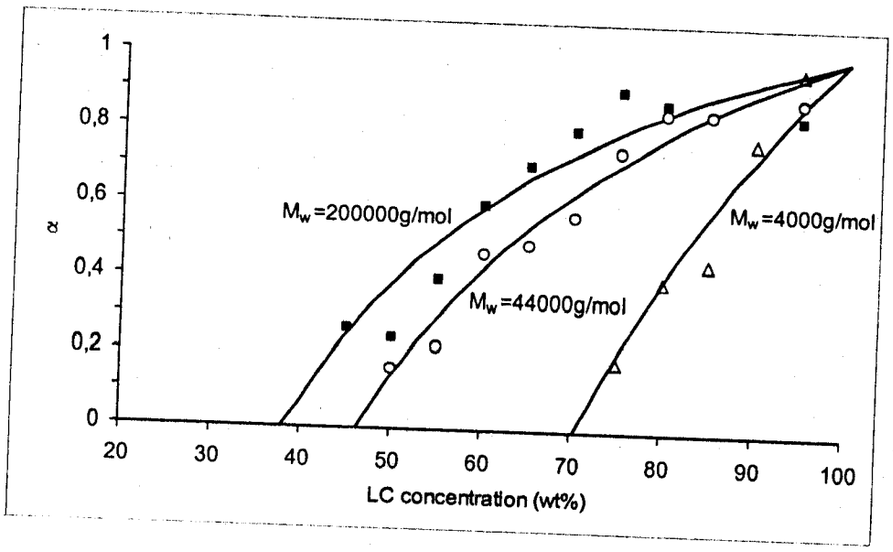

Figure 6

Fraction of 8CB in nematic droplets α obtained from ΔH_{NI} data versus total LC composition for the three molecular weights in the decreasing order from the top. The symbols ■, ○ and Δ represent the data for the three systems in the decreasing order of molecular weight determined by applying eq 27, whereas the solid lines were calculated by using the corresponding β values from Figure 5c and eq 26.

Figure 6 shows α versus φ_1 for the three systems under investigation. Clearly, similar informations are contained in the curves of ΔH_{NI} versus φ_1 (Figure 5) but Figure 6 has the merit of giving directly the amount of LC in the nematic domains and shows how this amount increases with the polymer size. These plots show that α can be quite large if the polymer size increases. In the case of low molecular weight polymer, α could be roughly

described by a linear segment, but as the polymer size increases, the data show that α first increases then tends to level-off as the concentration of LC becomes high. For a large size polymer, there is a strong increase of α below φ_1=0.7. Above this concentration, the value of α remains approximately constant indicating saturation of the polymer rich phase. This tendency is also seen for the intermediate size polymer but the concentration of LC where saturation is reached is higher.

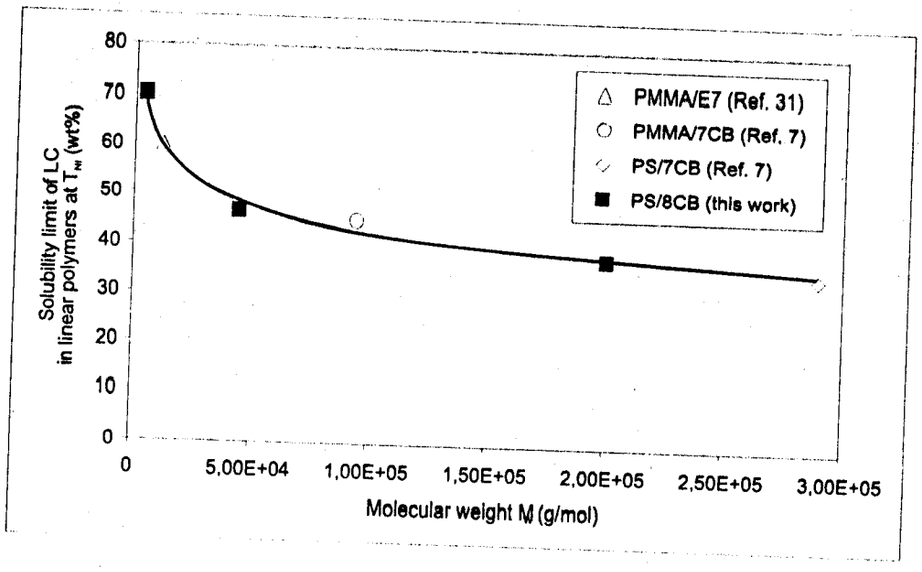

Figure 7

Experimental data showing the variation of α as a function of polymer molecular weight for different linear polymer/LC mixtures. The data shown here include results of the present work and results taken from the literature as indicated on the figure. The solid line is a least square fit to the data.

Figure 7 represents the variation of the solubility limit of the LC at T_{NI} with the polymer molecular weight. This plot includes data of the present work and other data published in the literature for other mixtures of linear polymers and low molecular weight LC.[7,31] Although these systems involve different polymers and different LC, the results fall on the same master curve. Beyond a certain polymer size, the solubility of the LC in the polymer

reaches a plateau limit. If such a variation is confirmed, then this result would allow prediction of the solubility limit of other systems. This could have important consequences since it would mean that beyond a certain polymer molecular weight the nature of the species in the mixture is irrelevant as long as α is concerned.

5. Conclusions

The phase behavior of PS/8CB mixtures with three molecular weights of the polymer different by two orders of magnitude is studied both experimentally and theoretically. The experimental data are obtained using POM, LS, and DSC and allow construction of the complete phase diagrams for the three systems. These diagrams exhibit several regions: At low temperatures, a miscibility gap consisting of an isotropic polymer rich phase coexisting with a smectic LC phase is observed for all molecular weights. At temperatures above 33.5°C, there is a transition from smectic to nematic order and one obtains an (N+I) biphasic region for the three systems. Above 40.5°C, the LC in the ordered phase becomes isotropic but the transition depends strongly on the polymer size. For the two highest molecular weights, the phase diagrams show an (I+I) miscibility gap while for the lowest molecular weight, a direct transition from (N+I) to a single isotropic I phase is found. Clearly the latter system exhibits a much higher solubility of the LC in the polymer than the other systems considered here. This enhanced compatibility is expressed not only by the absence of an (I+I) gap but also by a significant shift of the cloud point curve to the right leaving a much wider region for the single I phase.

The experimental phase diagrams are analyzed with the theoretical framework combining the Flory-Huggins theory of isotropic mixing and the Maier-Saupe theory of nematic order generalized by McMillan to include smectic-A order. Good agreement is obtained between experimental data and theoretical predictions.

In addition to phase diagrams the thermophysical properties obtained from DSC measurements were analyzed according to the procedure suggested by Smith.[29,30] Both enthalpy changes in the (S-N) and (N-I) transitions were examined to deduce solubility limits of the LC in the polymer. The data for ΔH_{SN} are not sufficiently accurate to allow for reliable predictions on the solubility properties. However, the enthalpy changes in the (N-I)

transitions are much more significant and were used successfully to obtain with good accuracy the solubility limits and the amount of LC dissolved in the polymer. In particular, the effect of polymer molecular weight on these thermal properties were unambiguously identified via a miscibility loss with increasing molecular weight. A single curve representing the solubility limit versus polymer molecular weight for several systems is obtained. This result allows one to make predictions on other systems with different polymers and LCs without having to make additional measurements. The curve of the solubility limit at T_{NI} versus molecular weight shows a sharp decrease for relatively low M_w followed by a leveling-off indicating saturation of the polymer rich phase. This phenomenon might be related to the formation of a physical network due to a strong entanglement of polymer chains as the molecular weight increases. To our knowledge this is the first time that such observations are made on the variation of the solubility limit of polymer/LC mixtures with the size of the polymer. It is evident that further studies will be necessary to understand the relationship between the solubility limit of the LC and the polymer molecular weight.

References

1. Doane, J. W. Polymer Dispersed Liquid Crystal Displays. In: *Liquid Crystals: Their Applications and Uses*; Bahadur, B.; Ed.; World Scientific: Singapore, 1990.
2. Drzaic, P. S. *Liquid Crystal Dispersions*; World Scientific: Singapore, 1995.
3. *Liquid Crystals in Complex Geometries*; Crawford, G P., Zumer S.; Eds.; Taylor&Francis: London, 1996.
4. Maschke, U.; Coqueret, X.; Loucheux, C. *J. Appl. Polym. Sci.* **1995**, *56*, 1547.
5. Smith, G. W. *Mol. Cryst. Liq. Cryst.* **1990**, *180B*, 201.
6. Russell, G. M.; Paterson, B. J. A.; Imrie, C. T.; Heeks, S. K. *Chem. Mater.* **1995**, *7*, 2185.
7. Ahn, W.; Kim, C. Y.; Kim, H.; Kim, S. C. *Macromolecules* **1992**, *25*, 5002.
8. Maschke, U.; Roussel, F.; Buisine, J.-M.; Coqueret, X. *J. Therm. Anal. Cal.* **1998**, *51*, 737.
9. Roussel, F.; Buisine, J.-M.; Maschke, U.; Coqueret, X. *Mol. Cryst. Liq. Cryst.* **1997**, *299*, 321.
10. Maschke, U.; Turgis, J.-D.; Traisnel, A.; Coqueret, X. *Mol. Cryst. Liq. Cryst.* **1996**, *282*, 407.
11. Gyselinck, F.; Maschke, U.; Traisnel, A.; Coqueret, X. *Mol. Cryst. Liq. Cryst.* **1999**, *329*, 1181.
12. Kyu, T.; Shen, C.; Chiu, H.-W. *Mol. Cryst. Liq. Cryst.* **1996**, *287*, 27.
13. Kim, W.-K.; Kyu, T. *Mol. Cryst. Liq. Cryst.* **1994**, *250*, 131.
14. Benmouna, F.; Daoudi, A.; Roussel, F.; Buisine, J.-M.; Coqueret, X.; Maschke, U. *J. Polym. Sci., Part B: Physics Ed.* **1999**, *37*, 1841.
15. Flory, P. J. *Principles of Polymer Chemistry*; Cornell University Press: Ithaca, NY, 1965.

16. Maier, W.; Saupe, A. *Z. Naturforschung* **1959**, *14a*, 882.

17. Maier, W.; Saupe, A. *Z. Naturforschung* **1960**, *15a*, 287.

18. McMillan, W. L. *Phys. Rev. A*, **1971**, *4*, 1238.

19. De Gennes, P. G.; Prost, J. *The Physics of Liquid Crystals*, Oxford Science Publications, Clarendon Press: Oxford, U.K., 1994.

20. Chandrasekhar, S. *Liquid Crystals*, 2nd ed.; Cambridge University Press: Cambridge, U.K.,1992.

21. Gray, G. W.; Goodby, J. W. *Smectic Liquid Crystals: Textures and Structures*, Leonard Hill, Heyden & Son Inc.: Philadelphia, 1984.

22. Kyu, T.; Chiu, H.-W. *Phys. Rev. E* **1996**, *53*, 3618.

23. Chiu, H.-W.; Kyu, T. *J. Chem. Phys.* **1997**, *107*, 6859.

24. Chiu, H.-W.; Kyu, T. *J. Chem. Phys.* **1998**, *108*, 3249.

25. Kyu, T.; Liang, S.; Chiu, H.-W. *Macromolecules* **1998**, *31*, 3604.

26. Matsuyama, A.; Kato, T. *J. Chem. Phys.* **1998**, *108*, 2067.

27. Benmouna, F.; Coqueret, X.; Maschke, U.; Benmouna, M. *Macromolecules* **1998**, *31*, 4879.

28. Leclercq, L., Maschke, U.; Ewen, B.; Coqueret, X.; Mechernene, L; Benmouna, M. *Liq. Cryst.* **1999**, *26*, 415.

29. Smith, G. W.; Vaz, N. A. *Liq. Cryst.* **1988**, *3*, 543.

30. Smith, G. W.; Ventouris, G. M.; West, J. L. *Mol. Cryst. Liq. Cryst.* **1992**, *213*, 11.

31. Challa, S. R.; Wang, S. Q.; Koenig, J. L. *J. Therm. Anal. Cal.* **1995**, *45*, 1297.